# SEMI-ANNUAL REPORT

**TITLE OF GRANT:**

Electronic Characterization of Defects in Narrow Gap Semiconductors - Comparison of Electronic Energy Levels and Formation Energies in Mercury Cadmium Telluride, Mercury Zinc Telluride, and Mercury Zinc Selenide

**NAME OF PRINCIPAL INVESTIGATOR:**

James D. Patterson
James D. Patterson

**NAME OF POST DOCTORAL RESEARCH ASSOCIATE:**

Wei-Gang Li
Wei-Gang Li

**PERIOD COVERED BY THE REPORT:**

September 19, 1994 to March 19, 1995
(Mid Year Report)

**NAME AND ADDRESS OF GRANTEE INSTITUTION:**

Florida Institute of Technology
150 West University Boulevard
Melbourne, FL 32901
(INDEX Number: 9441)

**GRANT NUMBER:**

GP29-NAG8-1094
George C. Marshall Space Flight Center
Marshall Space Flight Center, AL 35812
(Technical Officers: Sharon Cobb, ES75, Sandor L. Lehoczky, ES75)

# OUTLINE

# I. INTRODUCTION

## A. Previous Work

It seems that this is a good moment to review how we got to where we are. During the summers of 1987 and 1988 the Principal Investigator (JDP) went to Marshall Space Flight Center to participate as a NASA/ASEE Fellowship program working for Dr. S.L. Lehoczky in the microgravity section of the Space Science Laboratory. Two reports and one publication ensued [1-3]. This was followed by a grant from the Space Research Institute at Florida Tech and by four grants from NASA/Marshall. Each grant was in excess of $30K and has supported graduate students, post docs, and travel. The grants have enabled me to be continuously supported from 1989 to the present date. Five more publications, one Ph.D. thesis, four reports, and seven presentations have resulted [4-19]. In addition, three general interest articles have appeared [20-22]. The original direction of our work was to use and extend the electron mobility work (as best exemplified by a long program) of Dr. S.L. Lehoczky. The work has been enlarged to include other areas as indicated below.

## B. Current Work

The project has evolved to that of using Green's functions to predict properties of deep defects in narrow gap materials. Deep defects are now defined as originating from short range potentials and are often located near the middle of the energy gap. They are important because they affect the lifetime of charge carriers and hence the switching time of transistors. We are now moving into the arena of predicting formation energies of deep defects. This will also allow us to make predictions about the relative concentrations of the defects that could be expected at a given temperature.

The narrow gap materials Mercury Cadmium Telluride (MCT), Mercury Zinc Telluride (MZT), and Mercury Zinc Selenide (MZS) are of interest to NASA because they have commercial value for Infrared detecting materials, and because there is a good possibility that they can be grown better in a microgravity environment. The uniform growth of these crystals on earth is difficult because of convection (caused by solute depletion just ahead of the growing interface, and also due to thermal gradients). In general it is very difficult to grow crystals with both radial and axial homogeneity.

## II. DEFECTS IN COMPOUND SEMICONDUCTORS

### A. Types of Defects (Native and Impurity)

We start by naming the defects that we will be considering [23]. First we consider intrinsic defects. There are two antisite defects: an anion on a cation site $A_C$ and a cation on anion site $C_a$. There are two vacancies, an anion and a cation: ($V_a$, $V_c$). Finally there are four anion and cation tetrahedral site interstitials: $A(T_a)$, $A(T_c)$, $C(T_a)$, $C(T_c)$. By $T_a$ we mean a tetrahedral site surrounded by an anion, and by $T_c$ we mean a tretrahedral site surrounded by a cation. This adds up to eight intrinsic native defects.

We let X denote an extrinsic impurity defect. Two of them are substitutional: anion-site $X_a$ and cation-site $X_c$. Two are interstitial: anions $X(T_a)$ and cations $X(T_c)$. No other interstitital defect sites are considered as they would be of lower symmetry (e.g. hexagonal) and perhaps less likely. We summarize these in the table below.

| **Native Defect** | **Symbol** | **Number** |
|---|---|---|
| Antisite | $A_C$, $C_a$ | 2 |
| Vacancy | $V_a$, $V_c$ | 2 |
| Interstitial | $A(T_a)$, $A(T_c)$ $C(T_a)$, $C(T_c)$ | 4 |
| **Impurity Defect** | **Symbol** | **Number** |
| Substitutional | $X_a$, $X_c$ | 2 |
| Interstitial | $X(T_a)$, $X(T_c)$ | 2 |

### B. Charge States

Defect concentrations depend on several factors which include temperature, chemical potential, stoichiometry and the number of extrinsic impurities. The concentration of defects also depends on the reaction energies which in turn depend on the formation energies. We will more carefully distinguish these two concepts later, but for now we wish to mention that formation energies typically are of order 10 eV,

and that they depend on the charge state of the defect.

Charge states introduce complications and we follow Zunger [24] in defining some needed terms. Let $V_i$ be the impurity atom valence and $V_h$ be the host valence. The charge on the impurity (in units of the magnitude of the electronic charge) will be called q. In the case of compound semiconductors, we will have a host valence for both the anions and cations ($V_h^a$, $V_h^c$). The atomic number of the neutral impurity will be denoted by Z.

The core electrons of the impurity number $Z - V_i$ and are regarded as inert. If we add n electrons to the impurity then $q = -n$ and the impurity has in effect $V_i - q = V_i + n$ valence electrons. $V_h$ of these are used to satisfy host crystal bonds. These become inert. The remaining $N = V_i + n - V_h$ impurity electrons are not inert and Zunger labels them as "active".

An example is helpful. Let us consider Mercury Cadmium Telluride in which Zn replaces a Te and for which $q = -1$. Neutral Zn has a structure of $[Ar]3d^{10}4s^2$, but in the solid at a Te location we think of it as having ionicity 2 and hence having the structure $...4s^24p^2$. [Ar] means the electronic structure of the Noble gas Ar. Neutral tellurium has structure $[Kr]4d^{10}5s^25p^4$ but in the solid we think of it as having an ionicity of 2 and hence with the structure $5s^25p^6$. By $Z_n^-$ we will mean $[Ar]3d^{10}4s^24p^3$ which still has one less electron than the nominal host. For this case $N = 4 + 1 - 8 = -3$ or we have three active "holes."

C. Concentrations

Most of the details are spelled out in a paper by Jansen and Sankey [23]. They show for example that,

$$[A_C][C_a] = \exp - (1/kT)[Eu(A_C)+Eu(C_a)]$$

By $[A_C]$ we mean the concentration of anions on cation sites etc. The $Eu(A_C)$ and $Eu(C_a)$ are the formation energies of the two defects and their sum is the reaction energy. For the intrinsic situations to be discussed, there are seven equations which define seven reaction energies. However, there are eight formation energies for the intrinsic defects. The arbitrary constant can be fixed by adding a side condition such as setting the cation and anion site vacancy formation energies equal in their zero charge state.

A typical equation giving reaction energies is

$$Eu(A_C) + Eu(C_A) = E_\mu(N+1, N-1, A_C) + E_\mu(N-1, N+1\ C_a) - 2E\ (N, N),$$

where for example, $E_\mu(N+1, N-1; A_C)$ means the perfect crystal bcc supercell energy at the chemical potential $\mu$ with N+1 anions and N-1 cations and an anion on a cation site. The actual supercell energy $E_\mu(N+1, N-1; A_C)$ depends on the computed supercell energy $E_C(N+1, N-1; A_C^{+n})$ for the charge state n by

$$E_\mu(N+1, N-1; A_C) = E_C(N+1, N-1; A_C^{+n}) + n(E_V+\mu)$$

where $E_V$ is the valence band edge and $\mu$ is the chemical potential measured relative to $E_V$. In effect we are adding in the n electrons at the Fermi level.

## III. DEEP DEFECTS IN ONE DIMENSION

### A. Model

The model we talk about has been well discussed by Economu [25]. It is convenient to summarize here because it shows easily how Green's function calculations can be used to calculate defect levels. It will also give us a model for explaining how we will use the ideas of Haldane and Anderson to calculate the effects of charge states in more realistic circumstances. The use of classical molecular dynamics to calculate the effects of relaxation of neighbors has already been discussed[8].

$$H_o = \Sigma_m |m> \varepsilon_o <m| + V \Sigma'_{nm} |m><n| , \qquad \text{(IIIA.1)}$$

where $|m>$ are Wannier like functions for site m, $\varepsilon_o$ is an atomic energy and V characterizes the strength of hopping between sites. The prime means to sum only over nearest neighbors n and m.

The substitutional impurity in the perfect lattice will be represented by

$$H_1 = |\ell> \varepsilon <\ell| , \qquad \text{(IIIA.2)}$$

where $\varepsilon$ is the change in "strength" of the binding at the impurity, which assumed to be located at site $\ell$.

The unperturbed Hamiltonian $H_o$ can be diagonalized by going to the Bloch representation $|k>$. The relationship between the two can be written:

$$|k> = \frac{1}{\sqrt{N}} \Sigma_\ell \, e^{ik\ell} \, |\ell> , \qquad \text{(IIIA.3)}$$

where N is the number of lattice sites. We find

$$H_o|k> = E_k|k> , \qquad \text{(IIIA.4)}$$

where

$$E_k = \varepsilon_o + 2V\cos(ka). \qquad \text{(IIIA.5)}$$

This is the usual result for the tight binding approximation, with nearest neighbor interactions in one dimension. The band is of width

4V and is between $\varepsilon_o + 2V$ and $\varepsilon_o - 2V$.

B. Green Functions

Green's functions are readily used to predict energy levels when the perturbation due to the substitutional defect is included. The unperturbed and perturbed Green's functions are given by

$$G_o(z) = (z - H_o)^{-1} \qquad \text{(IIIB.1)}$$

$$G_o(z) = (z - H_o - H_1)^{-1} \qquad \text{(IIIB.2)}$$

In order to deal with singularities, the possibility of z having a small imaginary component is allowed.

It is easy to show that the two Green's functions are related by

$$G = [1 - G_o H_1]^{-1} G_o . \qquad \text{(IIIB.3)}$$

One can rewrite this expression in terms of a T matrix as

$$G = G_o + G_o T G_o , \qquad \text{(IIIB.4)}$$

where $$T = H_1 + H_1 G_o H_1 + H_1 G_o H_1 G_o H_1 , \qquad \text{(IIIB.5)}$$

Defining $$G_o(\ell,\ell) = \langle \ell | G_o | \ell \rangle , \qquad \text{(IIIB.6)}$$

it is then easy to show

$$T = |\ell\rangle \frac{\varepsilon}{1 - \varepsilon G_o(\ell,\ell)} \langle \ell| , \qquad \text{(IIIB.7)}$$

As a general property we know the poles of T (or G) correspond to the discrete eigenvalues of H. Calling these discrete eigenvalues $E_p$ we have

$$G_o\left(\ell,\ell,E_p\right) = \frac{1}{\varepsilon}. \qquad \text{(IIIB.8)}$$

From this, a plot of energy versus defect strength can be made.

It is beyond the scope of what we wish to do here, but it is easy to show

that the diagonal element of the unperturbed Green's function is

$$G_o(\ell,\ell,E_p)=\frac{1}{\sqrt{(E_p-\varepsilon_o)^2-(2V)^2}}, \qquad \text{(IIIB.9)}$$

In summary, the unperturbed Green function can be calculated once the band structure is known. Localized functions are used in the construction of the perturbed Hamiltonian from which a relationship can be derived between $G_o$ and the perturbation. The defect energy $E_p$, can then be calculated using the above equation. In three dimensions, similar results obtain. A tight binding Hamiltonian can be constructed by a fit to the actual band structure calculations and from this the perfect crystal Green's function is determined. This combined with a specification of the defect potential determines the energy level in the defect. The primary advantage of a Green's function calculation is that it treats an isolated defect in an otherwise perfect crystal with the same accuracy that one chooses to treat the corresponding perfect crystal.

## IV. CHARGE STATES

### A. Haldane and Anderson Approach in One Dimension

Each defect can exist in different charge states. The actual charge state of the defect may be unknown. The location of the energy level (in or out of the gap) is highly dependent on the charge state. This is especially true for narrow gap semiconductors. If we are going to deal with different charge states, we need to treat Coulomb interactions, which we will do by using ideas from Haldane and Anderson[26]. We will use the one dimensional model to gain some insight to the more general case.

The charge state splitting of a deep level in the band gap is the difference between the ionization energies of the impurity with charge q and the impurity with one or fewer electrons.

For the one dimensional model we had $G_o(\ell,\ell,E_p) = 1/\varepsilon$ and then by using the expression for G we find the defect energy is

$$E_p = \varepsilon_o - \sqrt{\varepsilon^2 + (2V)^2}\ , \qquad \text{(IVA.1)}$$

for the defect level below the band which is the only one considered.

In order to allow for different charge states we double the number of states by allowing each state to have a spin degeneracy corresponding to up or down spins.

$(\sigma = \pm 1/2)$. The perturbing Hamiltonian representing the substitutional impurity becomes

$$H_1 = \Sigma_\sigma\ |\ell\sigma>\ \varepsilon\ <\ell\sigma|\ . \qquad \text{(IVA.2)}$$

Following the usual assumptions of Hjalmarson, we determine ε by

$$\varepsilon = \beta(E_{imp} - E_{host})\ , \qquad \text{(IVA.3)}$$

where $E_{host}$ is the host atomic orbital energy $\varepsilon_o$, and $E_{imp}$ is the orbital energy of the atom which forms a defect in the substitutional case. $E_{host}$ and β are fixed empirical parameters, and by the theory of

Haldane and Anderson[26]

$$E_{imp} = a + bn_\ell , \tag{IVA.4}$$

where a and b are also empirical parameters. Because the levels are degenerate, we assume

$$m_{\ell,+1/2} = m_{\ell,-1/2} = m_\ell . \tag{IVA.5}$$

The Feynman-Hellman theorem can then be used to evaluate

$$m_\ell \propto |\langle d|\ell\rangle|^2 \propto \frac{\partial E}{\partial \varepsilon} , \tag{IVA.6}$$

with known proportionality constants.

We find for one electron that

$$E_{imp} - E_{host} = a - \varepsilon_0 + \frac{b}{2}\frac{\partial E}{\partial \varepsilon} , \tag{IVA.7}$$

and for two electrons

$$E_{imp} - E_{host} = a - \varepsilon_0 + b\frac{\partial E}{\partial \varepsilon} . \tag{IVA.8}$$

Using b' as b/2 for one electron and b for two electrons we have

$$\varepsilon = \beta\left(a - \varepsilon_0 + b'\frac{\partial E}{\partial \varepsilon}\right), \tag{IVA.9}$$

and

$$E = \varepsilon_0 - \sqrt{\varepsilon^2 + (2V)^2} . \tag{IVA.10}$$

These two equations can be solved self consistently. In one dimension this can be carried out analytically, but in three dimensions the situation is more complicated and the self consistency must be sought numerically. In one dimension, the charge state splitting is easily evaluated by looking at the difference of ionization energy in the one and two electron cases. See Figure A. We find as expected that the charged state interaction increases as the strength of the defect

increases.

B. Short Range and Coulomb Forces in Three Dimensions

It is worthwile to give another simplified example before we report results for real materials. We use an atom-like model with short range and Coulomb interactions to help us understand more about the relative importance of each type of interaction. A similar calculation without the sort range interaction has been presented by Lee et al[27].

Thus for one electron we assume,

$$H = -\frac{\hbar^2}{2m}\nabla^2 + V(r)\,, \tag{IVB.1}$$

where

$$V(r) = -V_o - \frac{\gamma}{r} \quad r < r_o \text{ and } \gamma^{-1} = 4\pi\varepsilon_o K\,, \tag{IVB.2}$$

and where K is the relative dielectric constant. Assuming

$$\psi = e^{-\alpha r}, \tag{IVB.3}$$

we obtain the approximate ground state energy by minimizing

$$E(\alpha) = \frac{\int \psi H \psi dV}{\int \psi^2 dV}\,. \tag{IVB.4}$$

Similarly for two electrons we write

$$H = -\frac{\hbar^2}{2m}\left(\nabla_1^2 + \nabla_2^2\right) + V(r_1) + V(r_2) + V_i(r_{12}) \tag{IVB.5}$$

where

$$V_i(r_{12}) = \frac{\gamma K}{r_{12}}\,, \tag{IVB.6}$$

and V(r) is the same as for the one electron case. Assuming $\psi = e^{-\alpha(r_1+r_2)}$ we obtain the approximate ground state energy by

minimizing

$$E(\alpha) = \frac{\int \psi H \psi \, dV_1 dV_2}{\int \psi^2 dV_1 dV_2} . \qquad \text{(IVB.7)}$$

Again the charge state splitting is obtained by looking at the difference in the ionization energy for the one and two electron cases.

As an example we show the charge state splitting as a function of the relative dielectric constant and well range for fixed well depth. See Figure B. As the relative dielectric constant approaches zero, the effect of the Coulomb tail becoms neglibile. Note that its effect flattens out fairly quickly. The decrease with $r_o$, the range of the short range potential, is presumably because the electrons can more easily avoid each other for large $r_o$.

For our actual calculations, we start from the basic ideas of Hjalmarson[28]. We add the spin-orbit interaction for the II-VI materials following the ideas of Kobayashi[29]. We also adapt the ideas of Lee[27] for charge states and follow the ideas of Haldane and Anderson for locating them. In addition, we adapt the work of Li[30, 31] and Myles to include relaxation effects.

Just as in the one dimensional case, the defect potential, the deep energy level and the charge density associated with the neighborhood of the impurity are determined self consistently. A $sp^3s^*$ tight binding model for electronic band structure with MCT treated in the virtual crystal approximation was used. As in all of these calculations, the chemical trends are expected to be much better predicted than actual exact energy levels. See Figure 1. Note that the effects of different charge states can be to move levels out of or into the band gap. Because our band gaps are very narrow, predicting whether the defect energy is in or out of the gap is very difficult. Relaxation, different charge states, or even different band structure calculation can change the position of the energy levels by more that the value of the band gap energy. Thus we have some confidence in our chemical trends predictions but not in absolute energy of the defect. More details follow.

C. Results for Realistic Models (no relaxation, relaxation, and relaxation plus different charge states)

I. Introduction

As already mentioned, the charged-state splitting of a deep level in the band gap is the difference between the ionization energies of the impurity with charge q and the impurity with one or more fewer electrons (or holes). That is, the charge-state splitting equals

$$\Delta E = E_c - E_n, \qquad \text{(IVC.1)}$$

where $E_c$ is the deep level produced by an impurity in the charged state and $E_n$ is the deep level produced by the same impurity in the neutral state.

The ionization energy of an impurity in a semiconductor is defined as the energy required to remove an electron (or hole) from the occupied deep level to the conduction (or valence) band.

The charged-state splitting of a deep level is a many-body effect which results from the Coulomb interactions among electrons. In simplified one-electron theories, the defect potential of an impurity is charge state independent since the theory ignores the interactions among electrons. However, in many electron theories or in effective one-electron theories of the mean field type, such as Hartree or Hatree Fock models, the defect potential is charge state dependent. Therefore, to study the effects of charged state splitting of deep levels we must use many-body or mean field theories.

We have used the Hjalmarson one-electron deep level theory to study the electronic properties of deep levels in many different semiconductor materials[8]. This simple theory gives good chemical trends of deep levels for many different kinds of defects in narrow gap semiconductors. But one of the disadvantages of this theory is that the charged-state splitting of deep levels is ignored since the effect of electron interactions are not included. However, we can combine Hjalmarson deep level theory with Haldane and Anderson model of Coulomb effects[26] to study the charged-state splitting of deep levels. The use of the Haldane and Anderson model enables us to include many-electron effects, while retaining much of the simplicity of Hjalmarson's theory. This idea has been successfully utilized by Lee, Dow, and Sankey to study charged-state splitting of deep levels in Si[27], by Sankey and Dow to treat interstitial levels in Si[32], and by Myles to treat substitutional impurities in MCT[31].

We want to use the same idea to study the effects of charged-state splitting of deep levels in narrow gap semiconductors. We will focus on the materials MCT (Mercury Cadmium Telluride), MZT(Mercury Zinc Telluride), and MZS (Mercury Zinc Sellenide).

## 2. Theory

As is well known, the presence of a point defect impurity breaks the translational symmetry of a perfect crystal and intoduces a perturbation into the one-electron Hamiltonian. The Schrodinger equation is

$$(H_o + V)\,|\psi> \;=\; E\,|\psi> \qquad \text{(IVC.2)}$$

The defect energy level E in the band gap of a semiconductor is given by non trivial solutions of the corresponding determinantal equation

$$\left(I - G^o(E)V\right)|\psi> \;=\; 0 \qquad \text{(IVC.3)}$$

Here $G^o(E) = (E - H_o)^{-1}$ is the Green's function of the host crystal.

In Hjalmarson's theory, the host crystal Hamiltonian $H^o$ is given by Vogl's band structure model as[8]

$$H_o = \Sigma\left(|ia\vec{R}> E_i^a <ia\vec{R}| + |jc\vec{R}^1> E_i^c <jc\vec{R}^1|\right) + \Sigma\left[|ia\vec{R}> V_{ij}^{ac} <jc\vec{R}^1| + h.c.\right] \qquad \text{(IVC.4)}$$

where a and c refer to anions and cations, $E_1^a$ and $E_1^c$ are on site parameters and $V_i^{ac}$ characterizes the nn interaction.

The defect potential is given by[8] (anion site)

$$V = \sum_i V_i = \sum_i |ia\vec{R}> U_i <ia\vec{R}| \qquad \text{(IVC.5)}$$

where i can be s, p or s* (for (4) or just s and p for (5))

$$U_i = \beta_i\left(E^i_{imp} - E^i_{host}\right); \qquad \text{(IVC.6)}$$

where $E_{imp}$ and $E_{host}$ are, respectively, the defect and host atomic orbital energies for states of symmetry i, and $\beta_i$ is an empirical parameter. In the simplest approximation, $E^i_{imp}$ is charge state independent. To include the effect of charged-state splitting of deep levels, we have to use Haldane and Anderson's model to compute the defect potential V.

The problem of determining the deep level energy E for a given charged state then has two parts: (i) finding E as a function of V by solving the determinant equation for a known $H^o$; (ii) determining the defect potential V for an appropriate charged state using Haldane and Anderson's model. Since (i) has been discussed in detail elsewhere[8], we only explain (ii) here.

Following Haldane and Anderson[26], for a free atom of ion in a given charged state, the atomic-orbital energies or ionization potentials in different charge states are given by

$$E_{s\sigma}\left(\{n_\alpha\}\right) = E^o_s + U_{ss}\sum_{\sigma'}{}' n_{s\sigma'} + U_{sp}\sum_{j,\sigma'} n_{p_j\sigma'} \qquad \text{(IVC.7)}$$

$$E_{p_i\sigma}\left(\{n_\alpha\}\right) = E^o_p + U_{pp}\sum_{j,\sigma'}{}' n_{p_j\sigma'} + U_{sp}\sum_{\sigma'} n_{s\sigma'} \qquad \text{(IVC.8)}$$

where $\sigma$ is the spin $(\uparrow$ or $\downarrow)$, i, j = x, y, or z and the prime on the summation indicates that the self-interaction (i = j and / or $\sigma = \sigma'$) is excluded. $n_{s\sigma}$ and $n_{p_i\sigma}$ are the occupation numbers (0 or 1) of the s orbital and $p_i$ orbitals of spin $\sigma$, respectively. $\alpha$ is one of the eight possible spin - orbitals $\left(\alpha = s\uparrow, s\downarrow, p_x\uparrow, p_x\downarrow, p_y\uparrow, p_y\downarrow, p_z\uparrow, \text{ or } p_z\downarrow\right)$. $\{n_\alpha\}$ is a collective set of occupation numbers. For example, if an atom has four outermost electrons, the collective set of $\{n_\alpha\}$ is $n_s\uparrow, n_s\downarrow, n_p\uparrow$, and $n_p\downarrow$. The parameters $U_{ss}, U_{pp}, U_{sp}$ represents the Coulomb repulsion between electrons in the same atom. The values of $E^o_s, E^o_p, U_{ss}, U_{pp}$, and $U_{sp}$ have been determined by Sankey and Dow for numerous atoms in Periodic

Table[32].

In the solid, we assume that the electronic energy of an atom is the same function of occupation numbers $n_{s\sigma}$ and $n_{pi\sigma}$ with the same empirical parameters, but the $n_{s\sigma}$ and $n_{pi\sigma}$ are not necessarily integers. As is well known, a point defect, in a tetrahedral site of a zinc blende material, has a point group of $T_d$. A deep level produced by such a defect can have either non-degenerate $A_1$ (s-like) symmetry or triply degenerate $T_2$ (p-like) symmetry. As suggested by Kobayashi, Sankey and Dow[29], including spin in the band structure but neglecting spin-orbit effects of the defect simply doubles the degeneracy of each level. That is, including spin in the calculation, we obtain two-fold degenerate $A_1$ levels and six-fold degenerate $T_2$ levels. Due to the degeneracy, we have $n_{A1} = n_{s\sigma}$ and $n_{T2} = n_{p,\sigma}$ for either spins $\sigma$. Therefore we can rewrite Eq. (7) and Eq. (8) as follows:

$$E_{A_1} = E_s^0 + U_{ss}\ n_{A_1} + 6U_{sp}\ n_{T_2} \qquad \text{(IVC.9)}$$

$$E_{T_2} = E_p^0 + 5U_{pp}\ n_{T_2} + 2U_{sp}\ n_{A_1} \qquad \text{(IVC.10)}$$

where $n_{A1}$ and $n_{T2}$ are occupation numbers of an electron on appropriate levels, and the self-interactions are excluded.

The spin-orbital occupation number $n_\mu (\mu = A_1 \text{ or } T_2)$ contains contributions from both the valence band and the deep levels. It can thus be written in the form

$$n_\mu = n_\mu^v + n_\mu^d \qquad \text{(IVC.11)}$$

where $n_\mu^v$ is the contribution from the redistribution of electrons in the valence band and $n_\mu^d$ comes from the occupied deep levels.

The valence-band portion of $n_\mu$ can be written as

$$n_\mu^v = -\int_{-\infty}^{0} F(E) D_\mu(E) dE \qquad \text{(IVC.12)}$$

where (at zero temperature) F(E) is unity if the one-electron state

of energy E is occupied and zero otherwise. $D_\mu(E)$ is the local density of states for the spin-orbital $\mu$, and we have taken the zero of energy at the valence band maximum. $D_\mu(E)$ is related to the Green's function of the host crystal, $G^o(E)$ and the defect potential V as follows

$$\begin{aligned} D(E) &= <\mu|\rho(E)|\mu> = -(1/\pi)I_m \\ <\mu|G(E)|\mu> &= -(1/\pi)I_m <\mu|[1-G_o V]G_o|\mu>, \end{aligned} \quad \text{(IVC.13)}$$

where $G(E)=[1-G_0(E)V]^{-1}G_0(E)$ is the Green's function including the defect, and $|\mu> = |ia\sigma>$ is the localized basis orbitals which $H^o$ is based on. Replacing Eq. (13) into Eq. (12) we have

$$n_\mu^v = \frac{1}{\pi} I_m \int_{-\infty}^{0} F(E) <\mu|G(E)|\mu> dE \qquad \text{(IVC.14)}$$

where $<\mu|G|\mu>$ is the diagonal element of Green's function G(E).

The contribution of the deep levels to the occupation number can be shown to be

$$n_\mu^d = \sum_i |<\mu|\varphi_i>|^2 , \qquad \text{(IVC.15)}$$

where i is the number of electrons on an appropriate state, ($A_1$ or $T_2$) and $|\varphi_i>$ is the defect wave function of an electron on an appropriate spin-orbital state. Considering the degeneracy, we have

$$n_{A1}{}^d = k|<A_1|\varphi>|^2 , \qquad \text{(IVC.16)}$$

where K can take a number among 0 to 2 depending on how many electrons are on the $A_1$ level, and

$$n_{T2}{}^d = m|<T_2|\varphi>|^2 , \qquad \text{(IVC.17)}$$

where m can take a value among 0 to 6 depending on how many electrons are on the $T_2$ levels.

It can be proved that[33]

$$|\langle\mu|\varphi\rangle|^2 = \frac{\partial E}{\partial U_\mu}, \qquad \text{(IVC.18)}$$

where $U_\mu$ is the diagonal element of defect potential V. If we ignore the effects of lattice relaxation, we can prove that

$$U_\mu = \frac{1}{G^\mu_{aa}}, \qquad \text{(IVC.19)}$$

where $G^\mu_{aa}$ is the diagonal element of the Green's function $G^o(E)$ for an appropriate state. Therefore

$$\frac{\partial E}{\partial U_\mu} = -\frac{|G^\mu_{aa}|^2}{\frac{\partial}{\partial E} G^\mu_{aa}}, \qquad \text{(IVC.20)}$$

and

$$|\langle\mu|\varphi\rangle|^2 = -\frac{|G^\mu_{aa}|^2}{\frac{\partial}{\partial E} G^\mu_{aa}}. \qquad \text{(IVC.21)}$$

Using Eq. (21), Eq. (16) and Eq. (17) can then be written as

$$n^d_{A_1} = -k\frac{|G^{A_1}_{aa}|^2}{\frac{\partial}{\partial E} G^{A_1}_{aa}}, \qquad \text{(IVC.22)}$$

and

$$n^d_{T_2} = -m\frac{|G^{T_2}_{aa}|^2}{\frac{\partial}{\partial E} G^{T_2}_{aa}}. \qquad \text{(IVC.23)}$$

Including the effects of lattice relaxation in the calculation can also be done (see Ref. 33). From Eq. (14) and Eq. (18), it is obvious

that the occupation number $n_\mu$ is dependent on deep level energy E and the defect potential V. In turn, the spin-orbital energies of a defect in the solid $E_i$(i=$A_1$ or $T_2$) in Eq. (9) and Eq. (10) are also dependent on E and V.

Now we can modify the defect potential V in Hjalmarson's theory and include the effects of charged-state splitting in our calculations. Instead of using atomic-orbital energies to compute $U_i$ in Eq. (6), we should use spin-orbital energies in Eq. (9) and Eq. (10) to compute $U_i$. That is now

$$U_{A_1} = \beta_{A_1}\left\{\left[E_S^o + U_{ss}\, n_{A_1} + 6U_{sp}\, n_{T_2}\right] - E_{host}^{A_1}\right\}, \qquad \text{(IVC.24)}$$

and

$$U_{T_2} = \beta_{T_2}\left\{\left[E_p^o + 5U_{pp}\, n_{T_2} + 2U_{sp}\, n_{A_1}\right] - E_{host}^{T_2}\right\}. \qquad \text{(IVC.25)}$$

Therefore $U_i$ is charged state dependent. It is worth pointing out that even though the off-diagonal elements in defect potential V keep in the same form, since for different charged states, the bond length between a defect and the surrounding host atoms is different, the off-diagonal elements of V are also charged state dependent[8].

Eqs. (14) and (18) give the dependence of the occupation numbers $n_\mu$ on the defect potential V and the deep level E. Conversely, Eqs. (24) and (25) give the dependence of V on the $n_\mu$. These equations form a set of coupled equations which must be solved self-consistently for the deep level energy E, defect potential V, the occupation number $n_\mu$, and the spin-orbital energies $E_\mu$. For a particular impurity, a scheme for obtaining self-consistent solutions for these quantities is implemented as follows: For a trial defect potential V which can be set to zero initially, Eq. (2) is solved for the deep level energy E. With this E and V, the occupation number $n_\mu$ are computed from Eq. (14), Eq. (22), and Eq. (23). These occupation numbers are then used to compute the spin-orbit energies from Eqs. (9) and (10). These energies are used to compute new defect potential V from Eqs. (24) and (25). This procedure is repeated iteratively until self-consistent is obtained.

As an example of the calculations, we consider a Zn atom substituting for Te in MCT for three charged states $Zn^0$, $Zn^-$,

$Zn^+$. The neutral impurity state $Zn^0_{Te}$ has four extra electrons relative to the host. The singly negatively charged impurity $Zn^-_{Te}$ has five extra electrons and the singly positively charged impurity $Zn^+_{Te}$ has three extra electrons. These extra electrons are expected to fill $A_1$ (s-like) level first and then $T_2$ (p-like) levels. In all these three charged states, we have a full $A_1$ level and an unfull $T_2$ level.

The occupation number $n_\mu$ is computed first. $n^v_\mu$ can be computed using Eq. (14) with V being zero initially. Then G(E) = $G^o(E)$ where $G^o(E)$ is the host Green's function which can be computed using the same method we used before. $n^d_\mu$ can be computed using Eqs. (22) and (23). For $n^d_{A_1}$, k is equal to two in all three charged states, and for $n^d_{T_2}$, m is equal to one, two, and three corresponding to three different charged states $Zn^+$, $Zn^0$, and $Zn^-$.
Then the spin-orbital energies $E_\mu$ are computed using Eq. (9) and Eq. (10). For a Zn atom, the values of the parameters are $E^o_s = -18.0, E^o_p = -11.9, U_{ss} = 10.0, U_{pp} = 7.8$, and $U_{sp} = 8.4$.[32] The diagonal elements $U_\mu$ of the defect potential V can then be computed using Eqs. (24) and (25). In the equation, $E_{host}$ are also parameters determined by Sankey. For a Te atom, $E_{host}$ of $A_1$ state is -19.0, and $E_{host}$ of a $T_2$ state is -9.8[32].

If we ignore the effects of lattice relaxation for different charged states, we can then use $U_\mu$ to construct a new defect potential V, and these new V, in turn, can be used to compute $n_\mu$. We assume that the self-consistency is achieved if

$$\Delta V = \left| \frac{\left(U^{in}_{A_1} - U^{out}_{A_1}\right) + \left(U^{in}_{T_2} - U^{out}_{T_2}\right)}{2} \right| < 10^{-3}. \qquad \text{(IVC.26)}$$

To study the shift of deep levels due to the different charged states, we first compute the deep level energies E as a function of $U_{A1}$ for $A_1$ deep levels and as a function of $U_{T2}$ for $T_2$ deep levels. For different charged states, we compute the corresponding $U_{A1}$ and $U_{T2}$ using the method discussed above. The charged state splitting can be obtained from the difference between the deep levels corresponding to different charged

states.

The results of calculations for our example above are as follows:

$Z^0$: $U_{A1} = 14.11$, $U_{T2} = 10.30$

$Z^-$: $U_{A1} = 15.74$, $U_{T2} = 11.11$

$Z^{--}$: $U_{A1} = 17.02$, $U_{T2} = 12.03$

$Z^+$: $U_{A1} = 12.39$, $U_{T2} = 9.17$

$Z^{++}$: $U_{A1} = 10.67$, $U_{T2} = 8.36$

Since the anion - site, s-like deep levels produced by Zn impurity in MCT are far away from the band gap, we just discuss the charged-state splitting of anion-site and p-like deep levels. The detail discussion about the results will be given in next section.

The effects of lattice relaxation can also be calculated simultaneously. To do that, for different defect potential V, we compute the corresponding defect bond length using the method we discussed before[33]. In turn, this will change the defect potential V. Therefore we need to include lattice relaxation when doing the calculation self-consistently. In many cases we found that the calculation of the lattice relaxation and the calculation of the charged-state splittings can be separated.

## 3. Results

Based on our theory, the electronic properties of deep levels in narrow gap semiconductors can be studied in three different stages. First, we focus on the chemical trends for the ordering of deep levels. To simplify the problem, the effects of lattice relaxation and the effects of charged state splittings are ignored. In the second stage we consider the relationship between deep levels and the lattice relaxation of the deep levels. The effects of lattice relaxation on deep levels are examined carefully. This work has been reported in the "Semi-Annual Report" [11] and the "Final Report" [12] last year. Here we consider charged state splittings of deep levels. The theory has been discussed in the last section.

The results from these three different stages are summarized in Fig. 1 for substitutional impurities of Zn and Mg in MCT. One can see from the figure that ignoring the effects of lattice relaxation and the effects of charged state splittings, an impurity Zn will produce a deep level in the middle of the band gap, and a deep level is formed in the lower half of the band gap by Mg. However, including the effects of lattice relaxation on deep levels, the deep level produced by Zn is shifted up to near the conduction band edge and the deep level formed by Mg is moved to the middle of the bad gap. If we assume that these two levels are formed by a neutral charged state (since we ignore the effects of charged state splittings in the second stage calculation), then we can use the method discussed above to compute the energy shift due to the charged states. It can be seen from the figure that the deep level produced by a singly negatively charged impurity $Zn^-$ is shifted to the conduction band. The energy shift between the charged state and the neutral state is about 0.12 eV. On the other hand, a singly positively charged impurity $Zn^+$ will move the deep level to the valence band. The corresponding energy shift is about 0.11 eV. Similar results can be found for impurity Mg. The neutral charged state $Mg^0$ is predicted to produce a deep level in the middle of the band gap. However, the singly negatively charged $Mg^-$ moves the level up to the conduction band with a shift about 0.08 eV, and a singly postively charged $Mg^+$ moves the level down to the valence band with a shift about the same amount. One can see from the figure that the effects of charged state splittings on deep levels are larger than the effects of lattice relaxation. This is true from our calculation for all defects of interest. Typically, the range of an energy shift due to the effects of lattice relaxation is 0.02 to 0.05 eV. However, the range of the energy shift due to the effects of charged state splittings is about 0.95 to 0.15 eV. Because the band gap of a narrow gap semiconductor is typically 0.1 eV, which is the same order as the charged state splittings, to predict a deep level formed by an impurity in the band gap, one must indicate the charged state of the impurity. It is easy to see that including the effects of charged state splittings of deep levels is very important to improve the deep level theory.

The results of charged state splittings of deep levels due to substitutional impurities in MCT, MZT, and MZS are summarized in Table 1. Five different charged states for each impurity, namely doubly positively charged state ($^{++}$), singly

positively charged state ($^+$), neutral charged state ($^0$), singly negatively charged state ($^-$), and double negatively charged state ($^{--}$) are considered. These different charged states have the meanings as follows: consider the charged states of impurity Zn substitutional for Te in MCT. Zn of any charge state has a deficit of four electrons compared with the Te it replaces. Two of these electrons will fill the s-like level, and the other two will fill the p-like level. Thus for $Zn^0$, which is what we call Zn with two more electrons than in the neutral atomic state, the s-like level will be full, and the p-like level will be partially full. Since $Zn^-$ has one more electron than $Zn^0$, this electron will go to the p-like level. On the other hand, since $Zn^+$ has one less electron than $Zn^0$, there is only one electron in the p-like level instead of two. For Zn with two less electrons than in the neutral state there will be a filled s-like level and an empty p-like level. Other impurities can be discussed in the same manner.

Even though the necessary information for calculating deep levels in all different situations (anion site, s-like; anion site, p-like; cation site, s-like; and cation site, p-like) are given in Table 1, we are only interested in anion site, p-like and cation site, s-like levels since the deep levels in the other two cases are far away from the band gap. Therefore, only anion site, p-like and cation site, s-like deep levels are considered in Table 1. Anion site, p-like levels produced by various charged states of Zn, Mg, Cd, and Hg, and cation site, s-like levels produced by S, Se, N, and Br in MCT are computed in the Table. The results of anion site, p-like levels produced by Zn, Mg, and Cd in MZT, and Zn, Mg, and Be in MZS are also given in the Table. In Table 1, the second column and the third column represent the impurity potential energy with appropriate symmetries (s-like or p-like) for different charged states of each impurity.

In the table, the fourth and the fifth column give the differences of impurity potential between the two charged states with one more or one less electron. The last column of the table shows the positions of corresponding deep levels relative to the band gap. For example, in the second row of the table, the impurity is Zn, and the charged state is singly negatively charged state ($Zn^-$). The impurity potential of $Zn^-$ in s-like and p-like states are 15.74 eV and 10.19 eV, respectively. The differences in impurity potential between $Zn^-$ and $Zn^0$ are 1.63 eV and 0.72 eV,

respectively. The position of the anion site, p-like deep level formed by $Zn^-$ is predicted at 2.1 Eg, where Eg is the energy band gap. Typically, the energy band gap is 0.1 eV, therefore, if a deep level is 0.9 Eg, it indicates that the deep level is in the band gap and below the conduction band edge by 0.1 x Eg eV. Therefore, the deep level formed by $Zn^-$ at 2.1Eg means that the deep level is at 2.1 x Eg eV, and is resonant in the conduction band. The charged state splittings $\Delta E$ can be obtained from the difference of deep levels between any two charged states for a particular impurity. For example, the charged state splitting between $Zn^-$ and $Zn^0$ is 0.12 eV, and between $Zn^0$ and $Zn^+$ is 0.11 eV.

The deep levels given in Table 1 are also shown in Fig. 2 to Fig. 5. In these figures, the bottom of the energy gap is at 0.0 eV and the top is at 0.1 eV. The deep levels formed by particular impurities with certain charged states are shown in these figures. Fig. 2 shows the anion site, p-like levels in MCT, and Fig. 3 shows the cation site, s-like levels in MCT. Fig. 4 and Fig. 5 represent the anion site, p-like levels in MZT and MZS, respectively. Some interesting observations can be found from these figures.

First the negatively charged impurities always form deep levels above those formed by the same impurities with neutral and positively charged states. The results can be explained qualitatively as follows. When the initially neutral impurity is given a single negative charge (an extra electron), the Coulomb repulsion of the extra electron with those already present will increase, as will the spin-orbital energy for the impurity, therefore the deep level energy will also increase. On the other hand, if the impurity is given a single positive charge by removing an electron The analagous resulting energies will decrease.

Second, it can be seen from the figures that the energy shift of the deep levels is roughly a linear function of the charged state for a particular impurity. That is the energy shift due to one more or one less electron in an impurity is roughly the same. For example, in Fig. 2, the energy shift from charged state $Zn^0$ to $Zn^-$ is 0.12 eV, and from $Zn^-$ to $Zn^{--}$ is also 0.12 eV. On the other hand, the energy shift from $Zn^0$ to $Zn^+$ is 0.1 eV, and from $Zn^+$ to $Zn^{++}$ is also 0.10 eV. In the case of impurity Mg, the

energy shift between charged states $Mg^{++}$, $Mg^{+}$, $Mg^{0}$, $Mg^{-}$, and $Mg^{--}$, are 0.07 eV, 0.07 eV, 0.08 eV, and 0.08 eV, respectively. That is, for different impurities, the energy shift between the same charged states may be different, but the energy shift between different charged states for the same impurity should be close.

Third, the chemical trends in the ordering of deep levels associated with different impurities for the same charged states are essentially unchanged. For example, the deep level produced by $Zn^{0}$ is above that produced by $Mg^{0}$, and the deep level formed by $Zn^{-}$ is also above that produced by $Mg^{-}$. However, the ordering of the deep levels associated with different impurities for different charged state may be changed. For instance, the deep level formed by Mg- is above that formed by $Zn^{0}$.

Table 2 summarizes the results for the interstitial impurities in MCT, MZT, and MZS. The meaning of each column in the Table is similar to that in Table 1. Five charged states are also considered for each impurity interested. One should notice that, however, in the case of interstitial impurities, the meaning of a neural state of an impurity is not the same as that of a substitutional impurity. The number of electrons on a neutral state of an interstitial impurity is the number of valence electrons of the impurity as an atom. For example, a neutral state of an interstitial impurity $Zn^{0}$ in MCT has two valence electrons instead of four as in the substitutional case for Te in MCT. These two electrons will be in the s-like deep level. Therefore, we have a filled s-like level and an empty p-like. A singly negatively charged state of $Zn^{-}$ has three extra electrons and the third electron will fill the p-like level. On the other hand, a singly positively charged state of $Zn^{+}$ has only one extra electron. Same discussion can be used for other interstitial impurities. The charged state splittings of an impurity can be easily obtained from the differences between two deep levels with different charged states.

Figs. 6-8 show the deep levels formed by various interstitial impurities with different charged states in MCT, MZT, and MZS. As before, the bottom of the band gap is at 0.0 eV and th top is at 0.1 eV. Inspecting these figures one can find that deep levels formed by interstitial impurities with different charged states have the similar properties as those formed by substitutional

impurities. For example, the deep levels are roughly a linear function of charged states; the negatively charged states have higher energy levels than neutral or positively charged levels; and the chemical trends of ordering of deep levels associated with different impurities for the same charged states are essentially preserved.

To illustrate these predictions, one can look at a specific example. Let's consider self-interstitial impurity Cd in MCT. One can see from Fig. 6 that the deep levels of five charged states formed by Cd ranging from '++' to '- -' are -2.4 Eg, -1.2 Eg, 0.8 Eg, 2.3 Eg, and 3.0 Eg, respectively. The corresponding energy shifts are 0.12 eV, 0.14 eV, 0.15 eV, and 0.15 eV. The most negatively charged state has the highest energy level. The energy shifts can be considered as a roughly linear function of the charged states.

Comparing the results of Table 1 with that of Table 2, one can see that the charged state splittings predicted for interstitial impurities are slightly higher than those predicted for substitutional impurities. For example, the charged state splittings of the substitutional impurity Zn in MCT are 0.1, 0.11, 0.12, and 0.12 eV when the charged states are changed from '++' to '- -'. However, the corresponding energies of the intersititial impurity Zn in MCT are 0.2, 0.22, 0.22, and 0.25 eV. Similar trends are found for other impurities. This is not surprising because of the fact that the interstitial's deep levels are more atomic than those of substitutional impurities.

The charged state splittings as a function of alloy composition x can also be studied. Table 3 gives the results of charged state splittings of anion site, p-like deep levels for Zn and Mg in MCT for x =0.2, x = 0.3, and x =0.5. In the Table, $\Delta E$ is the charged state splittings. As can be seen from the Table that, these splittings are of the same order of 0.1 eV for different x, and tend to decrease slightly with decreasing x.

## V. FORMATION ENERGIES

Extraction Energy $E_E$: This is the energy necessary to remove an atom from a bulk lattice site to a free atom site at the surface. We have assumed a Schottky defect which leaves behind a bulk vacancy [a Frenkel defect puts the freed atom in an interstitial position].

This extraction energy $E_E$ is easy enough in principal to calculate via

$$E_E = E_f - E_i$$

where $E_f$ = the total energy of a cluster of atoms with the central atom removed plus the energy recovered by placing the freed atom on a free atom surface site and $E_i$ = the total energy of the cluster before removal of the central atom.

For elemental semiconductors the vacancy formation energy is then simply

$$E_V = E_E - E_{cohesive}$$

where $E_{cohesive}$ is the bulk cohesive energy atom. For compound semiconductors the situation is more complicated. We have extraction energies for both anions and cations $\left(E_E^a, E_E^c\right)$. For average bonds, we find a vacancy formation energy as given by

$$E_V = \frac{1}{2}\left(E_E^a + E_E^c\right) - E_{cohesive}.$$

We have already studied the electronic properties of defects in narrow gap semiconductors, in some detail[8]. As mentioned, of particular interest in the nature of point defects, which consist of native vacancies, antisites, and interstitials, and extrinsic substitutional and interstitial impurities. One of the important predictions of the theory is that all these point defects may form deep levels in the energy band gap. Some kind of defects are easier to form in the band gap than other kinds. The next logical question one may ask is "can we compute the defect concentrations for a particular kind of point defect in a semiconduction?" Although the defect concentration depends on many factors such as stochiometry, temperature, chemical potential, etc., in many processes, the concentration is governed primarily by the defect formation energy. It is well known that the defect concentration depends exponentially on the defect formation energy[28]. Thus the

study of defect formation energy is of essential importance.

Calculations of the defect formation energies for substitutional or interstitial defects may be divided into two main categories. The first type of approach is the cluster calculations, which deal with a finite number of atoms around a defect. In this approach, the defect formation energy can be modeled as

$$E^f = E^t(\text{defect cluster}) - E^t(\text{perfect cluster}), \qquad (V.1)$$

where $E^t$ (defect cluster) is the total energy of a cluster containing the defect, and $E^t$ (perfect cluster) is the total energy of the host cluster without the defect[34]. The major disadvantage of such calculations is that the results may differ because of the choice of a cluster size or due to the boundary conditions at the surface of the cluster.

The second type of approach is based on the Green's function method, in which the periodicity of the host crystal is fully accounted for. We can still use the definition of the defect formation energy mentioned above. However, in order to compute the total energy, a cluster from the infinite crystal must be constructed. The idea of constructing a cluster from the host crystal is as follows: Considering the crystal with a defect, we start with one-electron Schrodinger equation. In the Green's function method this equation is transformed into a matrix equation, with a size determined by the size of the matrix of the perturbing potential due to the defect. In our theory the size of this defect potential matrix is used to determine the size of the cluster. If we want to include the effects of the second nearest neighbors of the defect in the defect potential matrix, the matrix has a size of 17 x 17 for diamond and zinc-blende semiconductors. The corresponding cluster, has a size of 17 atoms, which consists of a defect, four nearest neighbor atoms, and twelve second nearest neighbors. The bonds at the cluster edges are coupled to the infinite host crystal. That is, for the cluster without the defect, we keep the same values of tight binding parameters as in the infinite host crystal. For the cluster with the defect, the defect potential matrix will be included. In this approach the surfacelike states associated with the cluster boundary are then eliminated. As a matter of fact, this whole idea has been used to calclulate the deep levels in our previous work[8].

The total energy of a cluster with or without a defect can be modeled by

$$E^{tol} = E^{el} + E^r, \qquad (V.2)$$

where $E^{el}$ is the sum of the one-electron energies in the occupied states, and $E^r$ is the repulsive energy due to electron-electron repulsion and ion-ion repulsion and contains the correction for double counting contained in $E^{el}$. $E^{el}$ can be computed as follows:

$$E^{el} = \int_{-\infty}^{E_f} E\rho(E)dE, \qquad (V.3)$$

where $E_f$ is the Fermi energy and $\rho(E)$ is the electronic density of states. In the Green's function method we have

$$\rho(E) = -\frac{1}{\pi} \mathrm{Im} \mathrm{T\,r}\, G(E), \qquad (V.4)$$

where G(E) is the Green's function matrix. Therefore, Eq. (3) becomes

$$E^{el} = -\frac{1}{\pi} \mathrm{Im} \mathrm{T\,r} \int_{-\infty}^{E_f} E\, G(E)\, dE \qquad (V.5)$$

On the other hand, $E^r$ can be computed using Harrison's overlap interaction model from a pair potential as[35]

$$E^r = A'/d^4 \qquad (V.6)$$

where A′ is a proportionality constant, and d is the defect bond length.

In order to compute $E^{el}$ for a cluster without a defect, the host Green's function matrix $G^o(E)$ is used, otherwise, the Green's function matrix including a defect G(E) must be used. The computation of $G^o(E)$ and G(E) has been discussed in detail in our previous work. We focus now on how to determine the constant A′. From the Harrison model,

$$E^r(d) = \frac{21.3}{K}\left[\frac{h}{m}\right]^2 \frac{1}{|\varepsilon_h|}\frac{1}{d^4}, \qquad (V.7)$$

where $\varepsilon_h = \left(\varepsilon_s + 3\varepsilon_p\right)/4$ is the hybrid energy, and $\varepsilon_s$ and $\varepsilon_p$ are the atomic energy of s and p states, respectively. K is an empirical constant. Comparing Eq. (7) with Eq. (6), it can be seen that

$$A' = \frac{21.3}{K}\left[\frac{h}{m}\right]^2 \frac{1}{|\varepsilon_h|}. \qquad (V.8)$$

There is another way to determine A′ which is more natural and more accurate. The constant A′ can be determined from the equilibrium position of an atom in a perfect crystal. The detailed discussion of the problem has been made in our previous work[8]. The basic idea is as follows: The total force on an atom due to the surrounding atoms at certain direction can be modeled as:

$$F_x = F_x^a + F_x^r, \tag{V.9}$$

where $F_x^a$ and $F_x^r$ represent, respectively, the attractive part and repulsive part of the force. For the host crystal in the absence of the impurity, each atom is fixed at its perfect crystal equilibrium position and it must be true that

$$F_x^a = -F_x^r, \tag{V.10}$$

so that $F_X = 0$. Since

$$F_x^r = -\frac{\partial E^r}{\partial x}, \tag{V.11}$$

if we take x along the bond length direction, we then have

$$F_x^r = 4A'/d^5 = A/d^5. \tag{V.12}$$

That is A′ = A/4. Therefore, if we can determine A from Eq. (10), we can then determine A′ from the relation above.

As an example, let's consider the formation energy of a substitutional impurity Zn for Te in MCT. As well known that this impurity can form either s-like or p-like anion site deep levels in the band gap. Therefore the formation energy in these two states should be computed separately. Using the formula discussed above, the calculational results are as follows:

| | $E_s^{el}$(eV) | $E_s^r$(eV) | $E_s^t$(eV) | $E_p^{el}$(eV) | $E_p^r$(eV) | $E_p^t$(eV) |
|---|---|---|---|---|---|---|
| h.c. | -25.72 | 2.66 | -23.06 | -10.16 | 1.74 | -8.42 |
| imp.c. | -20.52 | 2.20 | -18.31 | -7.18 | 1.19 | -5.99 |

where h.c. means host crystal and imp c. means for the crystal with impurity.

As before the formation energy is represented as

$$E^f = E^t(\text{impurity cluster}) - E^t(\text{host crystal}).$$

From the results above, we have that

for s-like state, the formation energy is $E^f = 4.75$ eV
for p-like state, the formation energy is $E^f = 2.43$ eV.

The results indicate that the formation energy for a Zn to form a p-like deep level is much less than that for a Zn to form a s-like deep level. We can conclude that a substitutional impurity Zn will most likely form a p-like deep level than form a s-like level. In other words, the concentration of impurity Zn which forms p-like levels should be much larger than that of Zn which forms s-like levels.

## VI. REFERENCES


1. "Improving the Method of Calculating Electronic Properties of Narrow Bandgap Semiconductors," J.D. Patterson, NASA CR-179219, Marshall Space Flight Center, XXVII (1987).

2. "Electron Mobility in Mercury Cadmium Telluride," J.D. Patterson, NASA CR-183553, Marshall Space Flight Center, XXII (1988).

3. J.D. Patterson and S.L. Lehoczky, "The Second Born Approximation and the Freidel Sum Rule, "Physics Letters A, 137 (3), 137 (1989).

4. Wafaa Abdelhakiem, J.D. Patterson and S.L. Lehoczky, "A Comparison Between Electron Mobility in n-type $Hg_{1-x}Cd_xTe$ and $Hg_{1-x}Zn_xTe$." Materials Letters 11, 47-51 (1991).

5. J.D. Patterson, Wafaa A. Gobba and S.L. Lehoczky, "Electron Mobility in n-type $Hg_{1-x}Cd_x$ and $Hg_{1-x}Zn_xTe$ Alloys," Journal of Materials Science 7(8), 2211-2218 (1992).

6. Wafaa A. Gobba, J.D. Patterson and S.L. Lehoczky, "A comparison between electron mobilities in $Hg_{1-x}Mn_xTe$ and $Hg_{1-x}Cd_xTe$," Infrared Phys. 34, 311-321 (1993).

7. J.D. Patterson, "Narrow Gap Semiconductors," Condensed Matter News 3(1), 4-12 (1994).

8. W. Li and J.D. Patterson, "Deep Defects in Narrow-Gap Semiconductors," Phys. Rev. B 50, 14903-14910 (1994).

9. J.D. Patterson, "Improvement of Program to Calculate Electronic Properties of Narrow Band Gap Materials," NASA: Marshall Space Flight Center, Grant No. NAG8-781 (July 25, 1990) 269 pages.

10. J.D. Patterson, "Further Improvements in Program to Calculate Electronic Properties of Narrow Gap materials," NASA: Marshall Space Flight Center, Grant No. NAG8-781, Suppl 2 (September 15, 1992) 98 pages.

11. J.D. Patterson, "Electronic Characterization of Defects in Narrow Gap Semiconductors," NASA: Marshall Space Flight Center, Grant No. NAG8-941 (June 25, 1993) 54 pages.

12. J.D. Patterson, "Electronic Characterization of Defects in Narrow Gap Semiconductors," NASA: Marshall Space Flight Center Grant No. NAG8-941 (June 25, 1994), 54 pages plus Appendix.

13. W. Abdelhakiem and J.D. Patterson, "Calculation of Low Temperature Mobility in Semiconductors," Fl. Scientist 52 (suppl. 1) 34 (1989).

14. J.D. Patterson and Wafaa Abdelhakiem, "Free Electron Screening," Fl. Scientist 53, 33 (1990). Abstract of full paper which was presented at 1990 meeting of Florida Academy of Science.

15. Wafaa A. Gobba, J.D. Patterson and S.L. Lehoczky, "Electron Mobility in Mercury Zinc Telluride Alloys," Bull. Am. Phys. Soc. 37(1), 73 (1992).

16. J.D. Patterson and Wafaa A. Gobba, "Enhanced Screening in Doped Semiconductors," Bull. Am. Phys. Soc. 37(1), 196 (1992).

17. J.D. Patterson and Wafaa A. Gobba, "Electron Mobility in Mercury Manganese Telluride Alloys." Bull. Am. Phys. Soc. 38(1), 797 (1993).

18. W. Li and J.D. Patterson, "Deep Defects in Narrow Gap Semiconductors," Bull. Am. Phys. Soc. 38(1), 896 (1994).

19. Weigang Li and J.D. Patterson, "Theory of Deep Defects in Narrow Gap Semiconductors," Bull. Am. Phys. Soc. 40 510 (1995). Presented at March 1995 American Physical Society, San Jose, CA.

20. J. Patterson and S. Billings, "The Evolution of Space Science on the Space Coast," Brevard Technical Journal 1(5), 37 (1992).

21. J. Patterson and S. Billings, "Infrared: Light in the Dark," Brevard Technical Journal 1(9), 33 (1992).

22. J. Patterson, S. Billings, and J. Mantovani, "Space Grown Crystals," Brevard Technical Journal 2(8), 23 (1993).

23. Robert W. Jansen and Otto F. Sankey, "Theory of Relative Native - and Impurity - Defect Abundances in Compound Semiconductors and Factors That Influence Them," Phys. Rev. B 39, 3192-3206 (1989).

24. Alex Zunger, "Electronic Structure of 3D Transition Atom Impurities in Semiconductors," Solid State Physics 39, 275-464 (1986).

25. E.M. Economu, "Green's functions in Quantum Physics," Springer-Verlag, Berlin (1990).

26. F.D.M. Haldane and P.W. Anderson, "Simple Model of Multiple Charge States of Transition-Metal Impurities in Semiconductors," Phys. Rev. B 13, 2553-2559 (1976).

27. Seongbok Lee, John D. Dow, and Otto F. Sankey, "Theory of Charge-State Splittings of Deep Levels," Phys. Rev. B 31, 3910-3914 (1985). See also O.F. Sankey and J.D. Dow 27, 7641-7653 (1983).

28. H.P. Hjalmarson, P. Vogl, D.J. Wolford, and J.D. Dow, "Theory of Substitutional Deep Traps in Covalent Semicondutors," Phys. Rev. Lett. 44, 810 (1980).

29. Akiko Kobayashi, Otto F. Sankey, and John D. Dow, "Chemical Trends for Defect Energy Levels in $Hg_{(1-x)}Cd_xTe$," Phys. Rev. B 25 6367-6379 (1982).

30. Weigang Li and Charles W. Myles, "Deep-level wave functions including lattice-relaxation effects," Phys. Rev. B, 3281-4288 (1993).

31. Charles W. Myles, "Charge State Splitting of Deep Levels in $Hg_{1-x}Cd_xTe$," J. Vac. Sci. Technol A6 (4), 2675-2680 (1988).

32. O.F. Sankey and J.D. Dow, "Theory of tetrahedral-site interstitial s- and p-bonded impurities in Si," Phys. Rev. B 27, 7641-7653 (1983).

33. W. Li and C.W. Myles, "Deep-level wave functions including lattice-relaxation effects," Phys. Rev. B 47, 4281-4288 (1993).

34. Pan Bicai and Xia Shangda, "Formation Energy and Electronic Structure of Silicon Impurities in Diamond," Phys. Rev. B 49 (16), 11444-11447 (1994).

## VII. APPENDIX

### A. Some Brief Simple Facts

1. Cations are attracted to the Cathode and are positive. For our case examples are the Group II elements Hg and Cd.

2. Anions are attracted to the anode and are negative. Examples are Te and Se.

3. As far as lowering the potential energy goes, cation sites surrounded by negative ions tend to favor s-like levels (because this keeps negative charges as well separated as possible). Anion sites surrounded by positive ions tend to favor p levels which spread the negative charge out to the positive sites. Of course, covalent bonding and other effects can complicate this analysis.

4. Presumably because they are realtively compact, cation sites tend not to be affected by relaxation effects.

5. For substitutional impurities, atoms of Group II and to the left may replace anions (Group VI) and so according to the above like to be p type. Examples are $Mg_{Te}$ and $Be_{Se}$.

6. Similarly atoms of Group VI and to the right may replace cations (Group II) and so have neighbors which are negative and thus tend to be s-like impurities.

7. Substitutional sites are of Tetrahedral symmetry and interstitial sites can be Hexagonal and Tetrahedral. For interstitials we only consider Tetrahedral sites and name them in the same way as substitutional sites. For example, cation sites are surrounded by negative ions.

8. For a point defect in a tetrahedral site of a zinc blende material, the point group is Td. Such defects can have both non degenerate $A_1$ (s-like) and triply degenerate $T_2$ (p-like) states.

9. For our calculations, free atom parameters plus adjustment for being in the lattice define the diagonal part of the impurity potential.

10. The off diagonal part of the impurity potential is defined by a

constant determined by the host and the impurity, and by the host interatomic distance and the distance $d_I$, between the impurity and its nearest neighbors. The distance $d_I$, in the relaxed state is determined by molecular dynamics.

11. In our calculations, chemical trends seem to be preserved even though the aboslute energies are highly variable. For example, for substitutional levels caused by Cd, Zn, and Mg, we find the same order of levels in MCT, MZT, and MZS. As noted by Chen and Sher (Phys. Rev. B 31, 6490-6497 (1985)), the absolute location of the energy level may depend sensitively on the band structure and impurity potential. We also know it depends on relaxation and charge states. Particularly for a narrow gap semiconductor, the most we could hope to predict is chemical trends.

12. To standardize our calculation, we often use a band gap of 0.1 eV. The corresponding x values are x(MCT) = 0.22, x(MZT) = 0.15, and x(MZS) = 0.08.

13. The charged-state splitting of a deep level is a many body effect which results from the Coulomb interactions between electrons. The charged-state splitting of a deep level in the bad gap is the difference between the ionization energies of the impurity with charge q and the impurity with one fewer electron (or hole). The ionization energy of an impurity in a semiconductor is defined as the energy required to remove an electron (or hole) from the occupied deep level to the conduction (or valence band). We have used the ideas of Haldane and Anderson to approximately evaluate the charged-state splitting.

14. Simply put, the formation energy of a defect is the energy of the crystal with the defect less the perfect crystal energy. Defect concentrations depend exponentially on formation energies.

B. Selected references with titles and partial abstracts:

BI. Reviews

1. A. Sher, M.A. Berding, M. van Schilfgaarde and An-Ban Chen, "HgCdTe status review with emphasis on correlations, native defects and diffusion, " Semicond. Sci. Technol. 5 (1991) C59-C70. Printed in the UK.

Partial Abstract. The most vexing questions are about its correlation state, several different experiments now suggest it is highly correlated, but no theory predicts this result. The calculations predict that the main native defects found in alloys equilibrated at low Hg pressures are Hg vacancies, while at high Hg pressures they are Hg intersitials, and, surprisingly, Hg antisites.

2. C.E. Jones, K. James and J. Merz, R. Braunstein, M. Burd, and M. Eetemadi, S. Hutton and J. Drumheller, "Status of point defects in HgCdTe," J. Vac. Sci. Technol. A 3 (1), Jan/Feb 1985, p. 131.

Partial Abstract. Intrinsic defects such as the mercury vacancy, which is believed to act as a shallow acceptor, are less well understood and suffer from a lack of characterization techniques that can identify individual defects. Deep-level defects are present with concentrations proportional to the shallow acceptor concentrations. These centers often control lifetime and noise. At present, the errors in this work are larger than the HgCdTe band gaps, but the calculated trends are important.

3. Four Review Books

(a) S.T. Pantelides (Editor), "Deep Centers in Semiconductors," Gordon and Breach, Switzerland (1992).

(b) Ming-Fu Li, "Modern Semiconductor Quantum Physics," World Scientific, Singapore, 1994.

(c) Walter A. Harrison, "Electronic Structure and the Properties of Solids," W.H. Freeman and Co., San Francisco, 1980.

(d) W.A. Tiller, "The Science of Crystallization: microscopic interfacial phenomena and defect generation," Cambridge

University Press, 1991. "The Science of Crystallization: macroscopic phenomena and defect generation," Cambridge University Press, 1991.

BII. Relaxation

1. W. Li and J.D. Patterson, "Deep defects in narrow-gap semiconductors," Phys. Rev. B 50 (20), 15 November 1994, p. 14903.

Partial Abstract. The compounds considered are mercury cadmium telluride (MCT), mercury zinc telluride (MZT), and mercury zinc selenide (MZS). The effect of relaxation of neighbors is considered for the substitutional and intersitial cases. Although the absolute accuracy of our results is limited, the precision is good, and hence chemical trends are accurately predicted.

2. Wei-Gang Li and Charles W. Myles, "Deep-level wave functions including lattice-relaxation effects," Phys. Rev. B 47 (8), 15 Feb 1993, p. 4281.

Partial Abstract. A tight-binding formalism for calculating the wave functions associated with deep levels in semiconductors, including lattice relaxation effects, is presented. This formalism is an extension of the theory of Ren et al. [Phys. Rev. B 26, 951 (1982)] to include lattice relaxation.

3. Wei-Gang Li and Charles W. Myles, "Molecular-dynamics approach to lattice-relaxation effects on deep levels in semiconductors," Phys. Rev. B 43 (12), 15 April 1991, p. 9947.

Partial Abstract. Molecular dynamics is used to calculate the lattice relaxation around an impurity, and its efects on the associated deep levels are computed using a Green's-function method.

4. Wei-Gang Li and Charles W. Myles, "Effects of lattice relaxation on deep levels in semiconductors," Phys. Rev. B 43 (3), 15 Jan 1991, p. 2192.

Partial Abstract. A formalism for phenomenologically including the effects of nearest-neighbor lattice relaxation on deep levels associated with substitutional impurities in semiconductors is

outlined and used to investigate such effects in GaP and Si. This approach is an extension of the theory of Hjalmarson et al. [Phys. Rev. Lett. **44**, 810 (1980)].

BIII. Related to our Calculations

1. Charles W. Myles, "Charge state splittings of deep levels in $Hg_{1-x}Cd_xTe$," J. Vac. Sci. Technol. A6(4), p. 2675 (1988).

   Partial Abstract. The charge state splittings of the deep levels produced by a singly ionized, substitutional impurities on both the cation (Hg/Cd) and the ion (Te) sites in Hg1-xCdxTe are investigated using a Green's function formalism. In all cases investigated, the splittings are found to be of the order of 0.1 to 0.2 eV and to decrease with decreasing alloy composition (x).

2. Seongbok Lee and John D. Dow, "Theory of charge-state splittings of deep levels," Physical Reveiw B 31 (6), 15 March 1985, p. 3910.

   Partial Abstract. The Green's-function method, with an empirical tight-binding basis, is used to determine the deep levels of the singly ionized and neutral impurities S, Se, and Te in Si. The impurity potentials are determined self-consistently.

3. Otto F. Sankey and John D. Dow, "Theory of tetrahedral-site interstitial s- and p-bonded impurities in Si," Physical Review B 27 (12), 15 June 1983, p. 7641.

   Partial Abstract. A theory of the major chemical trends in the deep-energy levels of interstitial defects at the tetrahedral site in semiconductors is developed, based on a simple, empirical tight-binding scheme.

4. Akiko Kobayashi, Otto F. Sankey, and John D. Dow, "Chemical trends for defect energy levels in $Hg_{(1-x)}CdxTe$," Physical Review B 25 (10), 15 May 1982, p. 6357.

   Partial Abstract. The chemical trends for the energy levels of $sp^3$-bonded substitutional defects in Hg(1-x)CdxTe are predicted and appear to be in a general agreement with what is known about defect levels in this small-band gap semiconductor alloy.

5. F.D.M. Haldane and P.W. Anderson, "Simple model of multiple charge states of transition-metal impurities in semiconductors," Physical Review B 13 (6), 15 March 1976, p. 2553.

Partial Abstract. The Anderson model for magnetic impurities in metals is extended to semiconductors. It is shown how self-consistent Hartree-Fock solutions can exist in the gap for many different charge states of the impurity, providing the matrix elements coupling the impurity and substrate are large enough.

BIV. Interstitials

1. S. Goettig, "Localized interstitial states in tetrahedrally bonded semiconductors: The local-matrix approach," Physical Review B 42 (18), 15 December 1990, p. 11730.

Partial Abstract. An approach is presented for the localized states due to sp-type interstitials in tetrahedrally bonded crystals.

2. S. Goettig and C.G. Morgan-Pond, "Formation mechanisms of localized interstitial states in tetrahedrally bonded semiconductors," Physical Review B 42 (18), 15 December 1990, p. 11743.

Partial Abstract. The processes of formation of the localized defect states due to tetrahedral and hexagonal sp-type interstitials in sp-bonded materials are considered using a simple, tight-binding-type local matrix approach.

3. J.T. Schick and C.G. Morgan-Pond, "Point defects with lattice distortion in CdTe and HgCdTe," J. Vac. Sci. Tehnol., p. 1108 (1990).

Partial Abstract. Results of self-consistent, tight-binding supercell calculations of electronic defect levels and relaxation about defects for As, Sb, and Te interstitials in CdTe and for the Hg vacancy in HgTe are presented.

4. C.G. Morgan-Pond and J.T. Schick, S. Goettig, "Interstitial total energies and diffusion barriers in $Hg_{1-x}Cd_xTe$," J. Vac. Sci. AZ (2), p. 354 (1989).

Partial Abstract. The previous simple model used to calculate energy trends for the deep levels due to localized electronic states

associated with interstitial and substitutional defects has been extended to obtain estimates of the total energy for interstitials at different sites in the lattice. These calculations have been applied to predict the preferred tetrahedral site for Hg, Cd, In, and Te interstitials in $Hg_{1-x}Cd_xTe$, and to investigate a possible diffusion path for these interstitials.

5. S. Goettig and C.G. Morgan-Pond, "Deep interstitial levels in $Hg_{1-x}Cd_xTe$," J. Vac. Sci. Technol. A6 (4), p. 2670 (1988).
Partial Abstract. The deep levels of indium and self-interstitials (Hg, Cd, Te) in tetrahedral and hexagonal positions in $Hg_{1-x}Cd_xTe$ are characterized and energy trends are calculated within the defect-molecule approach.

BV. Vacancies

1. Y. Marfaing, "Point defects and defect-impurity interaction in $Cd_xHg_{1-x}Te$ and other II-VI semiconductors: Facts and conjectures," J. Vac. Sci. Technol. B 10(4), Jul/Aug 1992, p. 1444.

Partial Abstract. The properties of the cation vacancy in $Cd_xHg_{1-x}Te$ are re-examined in the light of two experiments (mass-loss measurements, positron lifetime) which point out to a large concenration of vacancy-type defects compared to the hole carrier density.

2. C. Blanchard and P. Girault, "Energy states of the cation vacancy in II-VI compounds," Semicond. Sci. Technol. 6 (1991) A 127-A130. Printed in the UK.

Partial Abstract. We have calculated, in the frame of a molecular model, the electronic states of the neutral, singly and doubly charged cation vacancy. We show that the ground state of a given charged vacancy is different depending on whether spin-orbit interaction is smaller or greater than the Coulomb repulsion potential.

3. M.A. Berding and A. Sher, A.B. Chen, "Vacancy formation and extraction energies in semiconductor compounds," J. Appl. Phys. 68 (10), 5064 (1990).

Partial Abstract. Extraction energies for diamond and zinc-blende semiconductor compounds and pseudobinary alloys are calculated using a tight-binding cluster method, where the final

state of the removed atom is in a free-atom state. For the elemental semiconductors, vacancy (for Schottky defect) formation energies, in which the final state of the removed atom is on the surface, have been calculated.

4. J. van der Rest and P. Pecheur, "Electronic structure of the ideal vacancies in Ge, GaAs and ZnSe crystals," J. Phys. C; Solid State 17, 85 (1984).

Partial Abstract. We study the electronic structure of the various charge states of the ideal vacancies in Ge, GaAs and ZnSe crystals in the tight-binding approximation.

NOTE: John-Teller (J-T) distortions can be important for vacant lattice sites. The J-T effects says systems having a degenerate (not due just to spin) ground state will spontaneously deform to lower the symmetry and also lower the energy.

BVI. Concentrations

1. Robert W. Jansen and Otto F. Sankey, "Theory of relative native- and impurity-defect abundances in compound semiconductors and the factors that influence them," Physical Review B 39 (5), 15 February 1989, p. 3192.

Partial Abstract. An ab initio pseudo-atomic-orbital method [Phys. Rev. B 36, 6520 (1987)] is used to predict relative point-defect abundances and the factors that influence them in a number of III-V and II-VI compound semiconductors. The concentrations are predicted from equilibrium statistical mechanics by making use of the defect-formation energies.

From Sher in Review Section

| Defect reaction | Defection concentration | Energy (eV) |
|---|---|---|
| $E_{V_{Hg}} + HgTe \leftrightarrow V_{Hg}Te + Hg_g$ | $[V_{Hg}] = P_{Hg}^{-1} K_{V_{Hg}}^{0} \exp(-E_{V_{Hg}} / kT)$ | 2.01† |
| $E_{Te_{Hg}} + 2HgTe \leftrightarrow Te_{Hg} + 2Hg_g$ | $[Te_{Hg}] = P_{Hg}^{-2} K_{Te_{Hg}}^{0} \exp(-E_{Te_{Hg}} / kT)$ | 4.53 |
| $E_{Te_i} + HgTe \leftrightarrow Te_i Te + Hg_g$ | $[Te_i] = P_{Hg}^{-1} K_{Te_i}^{0} \exp(-E_{Te_i} / kT)$ | 4.96 |

| | | |
|---|---|---|
| $E_{V_{Te}} + Hg_g \leftrightarrow HgV_{Te}$ | $[V_{Te}] = P_{Hg} K^0_{VTe} \exp(-E_{VTe} / kT)$ | 3.12‡ |
| $E_{He_{Te}} + 2Hg_g \leftrightarrow HgHg_{Te}$ | $[Hg_{Te}] = P^2_{Hg} K^0_{Hg_{Te}} \exp(-E_{Hg_{Te}} / kT)$ | -0.42 |
| $E_{He_i} - Hg_g \leftrightarrow Hg_1$ | $[Hg_1] = P_{Hg} K^0_{Hg_i} \exp(-E_{Hg_i} / kT)$ | 0.84, 0.98 |

† Corrected experimental number from Vydyanath [13,14].
‡ Calculated using a tight-binding Hamiltonian [17].

BVII. Experimental

1. G.M. Khattak and C.G. Scott, "Characteristics of deep levels in n-type CdTe," J. Phys.: Condens. Matter 3 (1991) 8619-8634. Printed in the U.K.

   Partial Abstract. Deep-level transient spectroscopy has been employed to study the defect states in n-type CdTe crystals subjected to a variety of annealing treatments. Several defects were interpreted as complex centres involving native defects and impurities.

2. M.C. Chen, M.W. Goodwin and T.L. Polgreen, "Deep levels in n-type HgCdTe," Journal of Crystal Growth 86 (1988) 484-489, North-Holland, Amsterdam.

   Partial Abstract. Deep levels in both bulk and LPE (liquid phase epitaxy) n-type $Hg_{0.685}Cd_{0.315}Te$ have been studied by deep level transient spectroscopy (DLTS) between 78 and 170 K using metal-insulator-semiconductor (MIS) capacitors.

3. R.E. Kremer and W.B. Leigh, "Deep levels in CdTe," Journal of Crystal Growth 86 (1988) 490-496, North-Holland, Amsterdam.

   Partial Abstract. We have used a variety of complementary techniques to study electronic trapping levels that are far from either band edge CdTe. These deep levels play an important role in determining the electrical properties of the material. Fifteen different levels have been identified as related to these impurities.

4. Charles W. Myles and P. Frazer Williams, R.A. Chapman and E.G. Bylander, "Identification of defect centers in $Hg_{1-x}Cd_xTe$ using their energy level composition dependence," J. Appl. Phys. 57 (12), 15 June 1985, p. 5279.

Partial Abstract. We have extended the Kobayashi, Sankey, and Dow [Phys. Rev. B 25, 6367 (1982)] theory of deep levels in $Hg_{1-x}Cd_xTe$ to include (vacancy, impurity) nearest-neighbor pairs. As an example, we compare our theoretical predictions for the dE/dx of levels associated with (vacancy, impurity) pairs to the experimental slopes of the energy levels observed in deep level transient spectroscopy by Jones, Nair, and Polla [Appl. Phys. Lett. 39, 248 (1981)] and find that the theory lends support to these workers' interpretation of their data.

BVIII. Sher (miscellany)

1. Srinivasan Krishnamurthy and Arden Sher, "Electron mobility in $Hg_{0.78}Cd_{0.22}Te$ alloy," J. Appl. Phys. 75 (12), 15 June 1994.

   Partial Abstract. The electron mobility in $Hg_{0.78}Cd_{0.22}Te$ is calculated by solving the Boltzmann transport equation with Fermi-Dirac statistics and a full band structure. The calculated values are in excellent agreement with experiments, and effects of various traditional approximations are discussed.

2. Arden Sher, An-Ban Chen, W.E. Spicer and C.K. Shih, "Defects influencing the structural integrity of semiconductors and their alloys," J. Vac. Sci. Technol. A 3 (1), Jan/Feb 1985, p. 105.

   Partial Abstract. The bond length and energy changes of the constitutents of alloys relative to their pure crystal values are calculated from an extension of Harrison's method. It is demonstrated that the already weak HgTe bonds are destabilized by adjacent CdTe, HgSe, but are stabilized by ZnTe.

3. A.B. Chen and A. Sher, "Sensitivity of defect energy levels to host band structures and impurity potentials in CdTe," Phys. Rev. B 32 (10), p. 6490.

   Partial Abstract. The sensitivity of defect energy levels in semiconductors to the host band structures and impurity potentials has been studied for approximately 30 impurities in CdTe using four different band-structure models. The discrepancies in the defect levels between two different sets of band structures and impurity potentials are found to range from less than 0.1 eV to the whole band gap (1.6 eV).

BIX. New Methods

1. Z.Q. Li and W. Potz, "Electronic density of states of semiconductor alloys from lattice-mismatched isovalent binary constituents," Phys. Rev. B 46 (4), 15 July 1992, p. 2109.

   Partial Abstract. The electronic DOS is calculated numerically via the recursion method. Results are presented for $ZnSe_{1-x}Te_x$.

2. Dieter J. Lohrmann and Lorenzo Resca, Giuseppe Pastori Parravicini, and Ronald D. Graft, "Shallow and deep impurity levels in multivalley semiconductors: A Green-function study of a cubic model by the recursion method," Phys. Rev. B 40 (12), 15 October 1989, p. 8404.

   Partial Abstract. We study by the recursion method impurity levels in a cubic model semiconductor with parameters corresponding to silicon. We also find that contributions to deep levels from the Coulombic tail of the impurity potential are substantially larger than the corresponding effective-mass-equation (EME) binding energies and cannot be treated perturbatively, at least for $Z \geq 2$.

3. Dieter J. Lohrmann and Lorenzo Resca, Giuseppe Pastori Parravicini, and Ronald D. Graft, "Shallow and deep impurity levels in multivalley semiconductors: A Green-function study of silicon by the recursion method," Phys. Rev. B. 40 (12), 15 October 1989, p. 8410.

   Partial Abstract. Shallow and deep impurity levels in silicon are studied by a single Green-function formalism based on the recursion method. The ability of this method to include arbitrary-range potentials without increasing the computational effort is illustrated. We first show that the recursion method accurately reproduces the results of the model of Hjalmarson et al. [Phys. Rev. Lett. 44, 810 (1980)] when only central-cell potentials are included.

C. Abstract Presented

Abstract Submitted
for the March 20-24, 1995 Meeting of the
American Physical Society

Session K15-DCMP: DEFECTS IN SEMICONDUCTORS: MOSTLY WIDE BANDGAP
Mixed session, Wednesday afternoon, March 22, 14:30
Room J1, San Jose Convention Center
K15.09

Theory of Deep Defects in Narrow Gap Semiconductors. Weigang Li, J.D. Patterson, Florida Institute of Technology -- We use a Green's function technique to calculate the position of deep defects in the narrow gap semiconductors mercury cadmium (MCT), mercury zinc telluride (MZT) and mercury zinc sellenide (MZS). Substitutional (including antisite), and interstitial (self and foreign) deep defects are considered. Relaxation effects are included and they can be greater for the interstitial case than the substitutional one. For all cases we find deep defects in the energy gap only for cation site s-like orbitals or anion site p-like orbitals, and for the substitutional case only the latter are appreciably effected by relaxation. For substitutional impurities in MCT, MZT, MZS, we consider x (the concentration of Cd or Zn) in the range $0.1 < x < 0.3$ and also for both substitutional and interstitial cases we do extensive calculations for x values appropriate to a band gap of 0.1 eV. For the substitutional case we find that I, Se, S, Rn, and N are possible defect candidates to form cation site, s-like levels in MCT and ZN and Mg are for anion site, p-like levels. Similarly in MCT for the interstitial case we find deep defect levels in the band gap for Au, Ag, Hg, Cd, Cu, and Zn for the cation site, and N, Ar, O, and F for the anion site. For the substitutional cases we have some examples where relaxation moves the levels into the band gap, whereas for interstitial cases we have examples where relaxation moves them out of the band gap. We find that the chemical trends of defect levels in MZT is similar to that in MCT, however, the same conclusion doesn't hold for MZS. The absolute accuracy of our results is limited, but the precision is good, and hence the chemical trends are accurately predicted. Supported by NASA Grant NAG8-941.

## D. Experimental and Theoretical Results

The most recent compilation of MCT work is C. Littler, "Deep Level Centres in HgCdTe," in Properties of Narrow-Gap Cadmium based Compounds," Edited by Peter Capper. INSPEC, the Institution of Electrical Engineers, London, U.K. 1994 (pp. 250-253).

Although deep defects have been studied for some time, a detailed understanding combining both theory and experiment is lacking in many cases.

As mentioned in Littler many experimental techniques have been developed to study deep levels. These include deep level transient spectroscopy, luminescence, electron spin resonance, Fourier Transform spectroscopy, and junction space-charge techniques. In what follows we show the comparisons to experiment that we have been able to do so far, and briefly review the calculations we have done.

*Reprinted from*

# PHYSICAL REVIEW B

## CONDENSED MATTER

15 NOVEMBER 1994
II

# Deep defects in narrow-gap semiconductors

W. Li and J. D. Patterson
*Physics and Space Sciences Department, Florida Institute of Technology, Melbourne, Florida 32901-6988*

pp. 14903-14910

*Published by*
THE AMERICAN PHYSICAL SOCIETY
*through the*
American Institute of Physics

Volume 50 Third Series Number 20

TABLE IV. Comparison of the predicted deep levels in MCT with experimental data.

| System | Deep levels Experiment | Theory[f] |
|---|---|---|
| $Hg_I$[a] (donor) | $0.7E_g$[b] (Ref. 18) | $0.83E_g$ |
| $Te_I$[a] (recom)[c] | $0.4E_g$ (Refs. 18 and 28) | $E_c$[d]+0.1 eV[e] |
| $Te_{Hg}$ (recom) | $0.4E_g$ (Refs. 18 and 28) | $E_c$+0.06 eV[e] |
| $Cu_{Te}$ (donor) | $0.5E_g$ (Ref. 29) | $E_c$+0.06 eV[e] |
| $Cu_{Te}$ (donor) | $E_c$+0.05 eV (Ref. 18) | $E_c$+0.06 eV[e] |
| $Au_{Te}$ (donor) | $0.8E_g$ (Refs. 18 and 29) | $E_c$+0.04 eV[e] |
| $Au_I$[a] (donor) | $0.8E_g$ (Refs. 18 and 29) | $0.91E_g$ |

[a]These are interstitial impurities.
[b]$E_g$ means energy band gap.
[c]Recombination center.
[d]$E_c$ means conduction-band edge.
[e]The difference between data and the theory result can be explained by the effects of charged-state splitting.
[f]The $x$ values for the experimental data here are in the range $0.2<x<0.3$. For our calculations, $x=0.22$. As seen in Fig. 1, the change in the energy levels for $0.2<x<0.3$ is very small and can be ignored for rough comparisons.

[18]C. E. Jones, K. James, J. Merz, R. Braunstein, M. Burd, M. Eetemadi, S. Hutton, and J. Drumheller, J. Vac. Sci. Technol. A **3**, 131 (1985).

[28]A. Sher, M. A. Berding, M. Van Schilfgaarde, and An-Ban Chen, Semicond. Sci. Technol. **6**, (1991).

[29]C. L. Littler, D. G. Seiler, and M. R. Loloee, J. Vac. Soc. A **8**, 1133 (1990).

| Substitutional Impurity | Neutral Atomic Configuration | Theory in Fraction of Eg |
|---|---|---|
| Anion Site p Impurity | | |
| Host MCT | | |
| Cd | $5s^2$ | CB |
| Mg | $3s^2$ | 0.5 |
| Zn | $4s^2$ | 0.9 |
| Hg | $6s^2$ | CB |
| Host MZT | | |
| Zn | $4s^2$ | 0.7 |
| Mg | $3s^2$ | 0.3 |
| Cd | $5s^2$ | CB |
| Hg | $6s^2$ | CB |
| Host MZS | | |
| Be | $2s^2$ | 0.6 |
| Ti | $6s^26p^1$ | 0.4 |
| In | $5s^25p^1$ | 0.3 |
| Hg | $6s^2$ | CB |
| Zn | $4s^2$ | CB |
| Cation Site s Impurity | | |
| Host MCT | | |
| Br | $4s^24p^5$ | 0.01 |
| N | $2s^22p^3$ | 0.14 |
| S | $3s^23p^4$ | 0.52 |
| Rn | $6s^26p^6$ | 0.55 |
| Se | $5s^25p^4$ | 0.87 |
| I | $5s^25p^6$ | 0.92 |
| Host MZT | | |
| N | $2s^22p^3$ | -0.1 |
| S | $3s^23p^4$ | 0.15 |
| Rn | $6s^26p^6$ | 0.21 |
| Se | $5s^25p^4$ | 0.27 |
| I | $5s^25p^6$ | 0.42 |

| | | |
|---|---|---|
| At | $6s^26p^4$ | 0.82 |
| Substitutional Impurity | Neutral Atomic Configuration | Theory in Fraction of Eg |
| Anion Site Impurity | | |
| Host MCT | | |
| Te | $5s^25p^4$ | CB |
| N | $2s^22p^3$ | 0.7 |
| O | $2s^22p^4$ | 0.6 |
| Ar | $3s^23p^6$ | 0.62 |
| F | $2s^22p^5$ | 0.24 |
| Host MZT | | |
| Te | $5s^25p^4$ | CB |
| N | $2s^22p^3$ | CB |
| O | $2s^22p^4$ | CB |
| Ar | $3s^23p^6$ | CB |
| F | | 0.5 |
| Host MZS | | |
| Se | $4s^24p^4$ | CB |
| N | $2s^22p^3$ | CB |
| O | $2s^22p^4$ | CB |
| F | $2s^22p^5$ | 0.4 |

| Substitutional Impurity | Neutral Atomic Configuration | Theory in Fraction of Eg |
|---|---|---|
| Cation Site s Impurity | | |
| Host MCT | | |
| Cd | $5s^2$ | 0.77 |
| Mg | $3s^2$ | CB |
| Zn | $4s^2$ | 0.1 |
| Hg | $6s^2$ | 0.83 |
| Au | $6s^1$ | 0.91 |
| Ag | $5s^1$ | 0.88 |
| Cu | $4s^1$ | 0.22 |
| Host MZT | | |
| Zn | $4s^2$ | 0.04 |
| Mg | $3s^2$ | 0.91 |
| Cd | $5s^2$ | 0.61 |
| Hg | $6s^2$ | 0.69 |
| Au | $6s^1$ | 0.55 |
| Ag | $5s^1$ | 0.71 |
| Cu | $4s^1$ | 0.3 |
| Host MZS | | |
| Hg | $6s^2$ | CB |
| Zn | $4s^2$ | 0.14 |
| Cd | $5s^2$ | 0.84 |
| Cu | $4s^1$ | 0.34 |
| Ag | $5s^1$ | CB |

E. Some Problems and Comments about Crystal Growth in Microgravity

1. Determine the effects of growth interface geometry on defect generation.

2. Determine the effect of solidification rate on defect generation.

3. (1) and (2) are ambitious because defect generation is really only empirically understood.

4. Defects seem to be generated near the solid-liquid interface and near the container wall. There, generation seems to be influenced by fluid-fluid flows which may be caused by temperature gradients and buoyancy caused convection.

5. For our materials, there is a wide separation of the liquidus and solidus curves. This will give a large segregation coefficient which will cause a difference in composition if the fluid immediately ahead of the interface depleted of solute from the nominal concentration. In turn, this causes buoyancy and convective flow mentioned in (4) as the HgTe rich component which is rejected during solidification is more dense.

6. Crystals tend to grow with both radial and axial inhomogeneity which can cause bandgap inhomogeneity.

7. It is hoped that several of these problems will be reduced in microgravity.

## F. Future Work

We only have calculated a few formation energies so far -- see Section V where we have exhibited a substitutional impurity as an example. We intend to do many more substitutional cases plus cases involving the formation energies of interstitials and vacancies. For vacancies we will start with a model which is close to the ideal vacancy model and try to generalize it. We would also hope to look at formation energies for different charge states.

With formation energies, we can make some predictions about what defects are most likely to be generated in the crystal growth process.

TABLE 1
Charge-state splittings of deep levels due to
substitutional impurities in MCT, MZT, and MZS with Eg = 0.1 eV

| impurity | VS(eV) | VP(eV) | $\|\Delta E_s\|$ | $\|\Delta E_p\|$ | Deep Levels |
|---|---|---|---|---|---|
| host MCT anion site | | | | | p-like levels |
| $Zn^{--}$: | 17.02 | 10.92 | 1.28 | 0.73 | 3.3Eg |
| $Zn^{-}$: | 15.74 | 10.19 | 1.63 | 0.72 | 2.1Eg |
| $Zn^{0}$: | 14.11 | 9.47 | ---- | ---- | 0.9Eg |
| $Zn^{+}$: | 12.39 | 8.70 | 1.72 | 0.77 | -0.2Eg |
| $Zn^{++}$: | 10.67 | 7.96 | 1.63 | 0.74 | -1.2Eg |
| $Mg^{--}$: | 15.23 | 8.11 | 1.22 | 0.43 | 2.1Eg |
| $Mg^{-}$: | 14.01 | 7.68 | 1.26 | 0.45 | 1.3Eg |
| $Mg^{0}$: | 12.75 | 7.23 | ---- | ---- | 0.5Eg |
| $Mg^{+}$: | 11.49 | 6.83 | 1.26 | 0.40 | -0.2Eg |
| $Mg^{++}$: | 10.23 | 6.44 | 1.26 | 0.41 | -0.9Eg |
| $Cd^{--}$: | 20.71 | 11.73 | 1.56 | 0.71 | 3.5Eg |
| $Cd^{-}$: | 19.15 | 11.02 | 1.58 | 0.68 | 2.3Eg |
| $Cd^{0}$: | 17.57 | 10.34 | ---- | ---- | 1.2Eg |
| $Cd^{+}$: | 15.91 | 9.66 | 1.66 | 0.72 | 0.1Eg |
| $Cd^{++}$: | 14.28 | 8.92 | 1.63 | 0.74 | -1.2Eg |

| | | | | | |
|---|---|---|---|---|---|
| $Hg^{--}$: | 22.93 | 14.55 | 1.92 | 1.02 | C.B. |
| $Hg^{-}$: | 21.01 | 13.53 | 1.92 | 1.03 | C.B. |
| $Hg^{0}$: | 19.09 | 12.50 | ---- | ---- | C.B. |
| $Hg^{+}$: | 17.14 | 11.44 | 1.95 | 1.06 | C.B. |
| $Hg^{++}$: | 15.03 | 10.17 | 2.11 | 1.27 | C.B. |
| cation site | | | | | s-like levels |
| $S^{--}$: | -17.23 | -8.67 | 1.82 | 1.07 | 1.7Eg |
| $S^{-}$: | -19.05 | -9.74 | 1.59 | 0.94 | 1.1Eg |
| $S^{0}$: | -20.64 | -10.68 | ---- | ---- | 0.6Eg |
| $S^{+}$: | -22.01 | -11.48 | 1.37 | 0.80 | 0.1Eg |
| $S^{++}$: | -24.42 | -12.54 | 2.11 | 1.06 | -0.6Eg |
| $N^{--}$: | -18.24 | -10.67 | 3.31 | 1.32 | 1.7 Eg |
| $N^{-}$: | -21.55 | -11.99 | 2.72 | 1.63 | 0.9Eg |
| $N^{0}$: | -24.27 | -13.62 | ---- | ---- | 0.2Eg |
| $N^{+}$: | -28.64 | -15.87 | 4.37 | 2.25 | -1.2Eg |
| $N^{++}$: | -32.98 | -17.94 | 4.34 | 2.07 | -2.2Eg |
| $Se^{--}$: | -15.22 | -6.07 | 1.23 | 0.7 | 1.6Eg |
| $Se^{-}$: | -16.45 | -6.77 | 1.32 | 1.2 | 1.2Eg |
| $Se^{0}$: | -17.77 | -7.97 | ---- | ---- | 0.8Eg |
| $Se^{+}$: | -19.21 | -8.78 | 1.44 | 0.81 | 0.3Eg |

| | | | | | |
|---|---|---|---|---|---|
| $Se^{++}$: | -20.62 | -9.61 | 1.41 | 0.83 | -0.8Eg |
| $Br^{--}$: | -28.06 | -15.15 | 2.11 | 1.18 | 1.3Eg |
| $Br^{-}$: | -30.17 | -16.33 | 2.13 | 1.26 | 0.7Eg |
| $Br^{0}$: | -32.30 | -17.59 | ---- | ---- | 0.1Eg |
| $Br^{+}$: | -34.21 | -18.60 | 1.91 | 1.01 | -0.4Eg |
| $Br^{++}$: | -35.72 | -19.50 | 1.51 | 0.90 | -0.8Eg |
| host MZT anion site | | | | | p-like levels |
| $Zn^{--}$: | 15.92 | 11.07 | 1.26 | 0.70 | 2.9Eg |
| $Zn^{-}$: | 14.66 | 10.37 | 1.23 | 0.66 | 1.7Eg |
| $Zn^{0}$: | 13.43 | 9.71 | ---- | ---- | 0.8Eg |
| $Zn^{+}$: | 12.45 | 9.27 | 0.98 | 0.44 | 0.0Eg |
| $Zn^{++}$: | 10.71 | 8.56 | 1.74 | 0.71 | -1.2Eg |
| $Mg^{--}$: | 14.18 | 8.5 | 0.90 | 0.46 | 1.8Eg |
| $Mg^{-}$: | 13.28 | 8.04 | 0.72 | 0.32 | 1.0Eg |
| $Mg^{0}$: | 12.56 | 7.72 | ---- | ---- | 0.5Eg |
| $Mg^{+}$: | 11.33 | 7.0 | 1.23 | 0.72 | -0.7Eg |
| $Mg^{++}$: | 10.37 | 6.32 | 0.97 | 0.68 | -1.8Eg |
| $Cd^{--}$: | 16.33 | 11.23 | 1.24 | 0.69 | 3.7Eg |
| $Cd^{-}$: | 15.09 | 10.54 | 1.23 | 0.68 | 2.6Eg |
| $Cd^{0}$: | 13.86 | 9.86 | ---- | ---- | 1.5Eg |

| | | | | | |
|---|---|---|---|---|---|
| $Cd^{+}$: | 12.81 | 9.39 | 1.05 | 0.47 | 0.6Eg |
| $Cd^{++}$: host MZS anion site | 11.58 | 8.67 | 1.23 | 0.72 | -0.9Eg p-like levels |
| $Zn^{--}$: | 12.35 | 5.59 | 1.73 | 0.85 | C.B. |
| $Zn^{-}$: | 10.62 | 4.74 | 1.59 | 0.98 | C.B. |
| $Zn^{0}$: | 9.03 | 3.76 | ---- | ---- | 1.9Eg |
| $Zn^{+}$: | 7.35 | 2.87 | 1.68 | 0.89 | 0.6Eg |
| $Zn^{++}$: | 5.52 | 1.77 | 1.83 | 1.10 | -0.8Eg |
| $Mg^{--}$: | 10.00 | 3.69 | 1.14 | 0.80 | C.B. |
| $Mg^{-}$: | 8.86 | 2.89 | 1.34 | 0.65 | C.B. |
| $Mg^{0}$: | 7.52 | 2.24 | ---- | ---- | 1.7Eg |
| $Mg^{+}$: | 6.26 | 1.51 | 1.26 | 0.73 | 0.4Eg |
| $Mg^{++}$: | 5.03 | 0.80 | 1.23 | 0.71 | -0.7Eg |
| $Be^{--}$: | 15.52 | 5.94 | 2.62 | 1.05 | 2.7Eg |
| $Be^{-}$: | 12.90 | 4.89 | 2.62 | 1.11 | 1.3Eg |
| $Be^{0}$: | 10.28 | 3.78 | ---- | ---- | 0.2Eg |
| $Be^{+}$: | 7.67 | 2.53 | 2.61 | 1.25 | -1.1Eg |
| $Be^{++}$: | 5.05 | 1.37 | 2.61 | 1.16 | -2.1Eg |

TABLE 2
Charge-state splittings of deep levels due to
interstitial impurities in MCT, MZT, and MZS with Eg = 0.1eV

| impurity | VS(eV) | VP(eV) | $\|\Delta E_s\|$ | $\|\Delta E_p\|$ | Deep Levels |
|---|---|---|---|---|---|
| host MCT cation site | | | | | s-like levels |
| $Zn^{++}$: | -16.73 | -12.70 | 2.34 | 0.97 | V.B. |
| $Zn^{+}$: | -14.39 | -11.73 | 2.47 | 0.98 | -2.1Eg |
| $Zn^{0}$: | -11.92 | -10.75 | ---- | ---- | 0.1Eg |
| $Zn^{-}$: | -9.36 | -9.77 | 2.56 | 0.98 | 2.3Eg |
| $Zn^{--}$: | -6.85 | -8.83 | 2.51 | 0.94 | C.B. |
| $Mg^{++}$: | -11.84 | -8.73 | 1.34 | 0.69 | -1.1Eg |
| $Mg^{+}$: | -10.50 | -8.04 | 1.30 | 0.63 | -0.1Eg |
| $Mg^{0}$: | -9.20 | -7.41 | ---- | ---- | 1.0Eg |
| $Mg^{-}$: | -7.87 | -6.74 | 1.33 | 0.67 | 2.1Eg |
| $Mg^{--}$: | -6.56 | -6.06 | 1.21 | 0.65 | 3.3Eg |
| $Cd^{++}$: | -14.65 | -10.64 | 1.74 | 0.96 | -2.4Eg |
| $Cd^{+}$: | -12.91 | -9.68 | 1.73 | 0.96 | -1.2Eg |
| $Cd^{0}$: | -11.18 | -8.72 | ---- | ---- | 0.8Eg |
| $Cd^{-}$: | -9.45 | -7.75 | 1.73 | 0.97 | 2.3Eg |
| $Cd^{--}$: | -7.73 | -6.82 | 1.72 | 0.93 | 3.8Eg |

| | | | | | |
|---|---|---|---|---|---|
| $Hg^{++}$: | -16.3 | -12.01 | 2.16 | 1.15 | -2.3Eg |
| $Hg^{+}$: | -14.14 | -10.86 | 1.92 | 1.16 | -0.6Eg |
| $Hg^{0}$: | -12.02 | -9.70 | ---- | ---- | 0.9Eg |
| $Hg^{-}$: | -9.85 | -8.56 | 2.17 | 1.14 | 2.6Eg |
| $Hg^{- -}$: | -7.72 | -7.41 | 2.13 | 1.15 | C.B. |
| | | | | | |
| $Be^{++}$: | -19.92 | -13.4 | 2.62 | 1.10 | V.B. |
| $Be^{+}$: | -17.30 | -12.3 | 2.62 | 1.11 | -1.8Eg |
| $Be^{0}$: | -14.68 | -11.2 | ---- | ---- | -0.1Eg |
| $Be^{-}$: | -12.07 | -10.1 | 2.61 | 1.10 | 1.8Eg |
| $Be^{- -}$: | -9.46 | -9.0 | 2.61 | 1.10 | C.B. |
| host of MZT cation site | | | | | s-like levels |
| $Zn^{++}$: | -10.87 | -9.02 | 0.86 | 0.57 | V.B. |
| $Zn^{+}$: | -10.01 | -8.45 | 0.98 | 0.64 | -2.3Eg |
| $Zn^{0}$: | -9.03 | -7.81 | ---- | ---- | -0.1Eg |
| $Zn^{-}$: | -8.12 | -7.11 | 0.70 | 0.91 | 1.9Eg |
| $Zn^{- -}$: | -7.31 | -6.63 | 0.48 | 0.81 | C.B. |
| | | | | | |
| $Mg^{++}$: | -9.87 | -7.21 | 0.53 | 0.54 | V.B. |
| $Mg^{+}$: | -9.34 | -6.67 | 0.62 | 0.42 | -0.7Eg |
| $Mg^{0}$: | -8.72 | -6.25 | ---- | ---- | 0.9Eg |

| | | | | | |
|---|---|---|---|---|---|
| $Mg^{-}$: | -8.05 | -5.77 | 0.67 | 0.48 | 1.8Eg |
| $Mg^{--}$: | -7.33 | -5.16 | 0.72 | 0.61 | C.B. |
| $Cd^{++}$: | -10.68 | -6.88 | 0.93 | 0.65 | V.B. |
| $Cd^{+}$: | -9.75 | -6.23 | 0.89 | 0.61 | -1.5Eg |
| $Cd^{0}$: | -8.86 | -5.62 | ---- | ---- | 0.6Eg |
| $Cd^{-}$: | -8.02 | -5.10 | 0.84 | 0.52 | 2.3Eg |
| $Cd^{--}$: | -7.34 | -4.73 | 0.68 | 0.33 | C.B. |
| $Hg^{++}$: | -11.05 | -8.11 | 1.23 | 0.68 | V.B. |
| $Hg^{+}$: | -9.82 | -7.43 | 1.02 | 0.65 | -1.6Eg |
| $Hg^{0}$: | -8.80 | -6.78 | ---- | ---- | 0.7Eg |
| $Hg^{-}$: | -7.98 | -6.22 | 0.82 | 0.55 | 2.1Eg |
| $Hg^{--}$: | -7.21 | -5.74 | 0.77 | 0.48 | C.B. |
| host of MZS cation site | | | | | s-like levels |
| $Zn^{++}$: | -14.43 | -10.68 | 1.82 | 1.12 | V.B. |
| $Zn^{+}$: | -12.61 | -9.71 | 1.79 | 0.96 | -1.5Eg |
| $Zn^{0}$: | -10.82 | -8.75 | ---- | ---- | 0.0Eg |
| $Zn^{-}$: | -9.21 | -7.67 | 1.61 | 0.87 | 1.7Eg |
| $Zn^{--}$: | -7.65 | -6.71 | 1.56 | 0.80 | C.B. |
| $Mg^{++}$: | -9.81 | -6.66 | 1.27 | 0.62 | -1.6Eg |

| | | | | | |
|---|---|---|---|---|---|
| $Mg^{+}$: | -8.54 | -6.04 | 1.31 | 0.70 | -0.1Eg |
| $Mg^{0}$: | -7.23 | -5.34 | ---- | ---- | 1.2Eg |
| $Mg^{-}$: | -5.97 | -4.64 | 1.27 | 0.70 | 2.5Eg |
| $Mg^{- -}$: | -4.76 | -4.06 | 1.21 | 0.58 | C.B. |
| $Cd^{++}$: | -11.68 | -7.54 | 1.76 | 0.96 | -2.6Eg |
| $Cd^{+}$: | -9.92 | -6.62 | 1.64 | 0.90 | -1.3Eg |
| $Cd^{0}$: | -8.18 | -5.72 | ---- | ---- | 0.9Eg |
| $Cd^{-}$: | -6.47 | -4.84 | 1.71 | 0.98 | 2.2Eg |
| $Cd^{- -}$: | -4.77 | -3.76 | 1.60 | 0.88 | C.B. |
| $Hg^{++}$: | -10.92 | -8.91 | 1.78 | 1.05 | V.B. |
| $Hg^{+}$: | -9.14 | -7.86 | 1.72 | 1.16 | -1.9Eg |
| $Hg^{0}$: | -7.42 | -6.70 | ---- | ---- | 0.0Eg |
| $Hg^{-}$: | -5.86 | -5.62 | 1.66 | 1.08 | 1.8Eg |
| $Hg^{- -}$: | -4.22 | -4.51 | 1.62 | 1.09 | C.B. |
| $Be^{++}$: | -14.98 | -11.04 | 2.18 | 1.01 | V.B. |
| $Be^{+}$: | -12.80 | -10.03 | 2.19 | 1.03 | -2.7Eg |
| $Be^{0}$: | -10.61 | -9.00 | ---- | ---- | -0.1 Eg |
| $Be^{-}$: | -8.47 | -8.03 | 2.14 | 0.97 | 1.8Eg |
| $Be^{- -}$: | -6.26 | -7.06 | 2.21 | 0.97 | C.B. |

TABLE 3
Comparison of charge-state splittings for x=0.2, 0.3, and 0.5 in MCT

| impurity | deep levels (anion site, p-like) | | | ΔE | | |
|---|---|---|---|---|---|---|
| | x=0.2 | x=0.3 | x=0.5 | x=0.2 | x=0.3 | x=0.5 |
| $Zn^{--}$: | 3.3Eg | 3.3Eg | 3.4Eg | 0.12 | 0.11 | 0.11 |
| $Zn^{-}$: | 2.1Eg | 2.2Eg | 2.3Eg | 0.12 | 0.13 | 0.13 |
| $Zn^{0}$: | 0.9Eg | 0.9Eg | 1.0Eg | ---- | ---- | ---- |
| $Zn^{+}$: | -0.2Eg | -0.2Eg | -0.1Eg | 0.13 | 0.13 | 0.11 |
| $Zn^{++}$: | -12.Eg | -1.1Eg | -1.0Eg | 0.10 | 0.11 | 0.09 |
| $Mg^{--}$: | 2.1Eg | 2.1Eg | 2.2Eg | 0.08 | 0.08 | 0.09 |
| $Mg^{-}$: | 1.3Eg | 1.3Eg | 1.3Eg | 0.08 | 0.08 | 0.07 |
| $Mg^{0}$: | 0.5Eg | 0.5Eg | 0.6Eg | ---- | ---- | ---- |
| $Mg^{+}$: | -0.2Eg | -0.2Eg | -0.1Eg | 0.07 | 0.07 | 0.07 |
| $Mg^{++}$: | -0.9Eg | -0.9Eg | -0.8Eg | 0.07 | 0.07 | 0.07 |

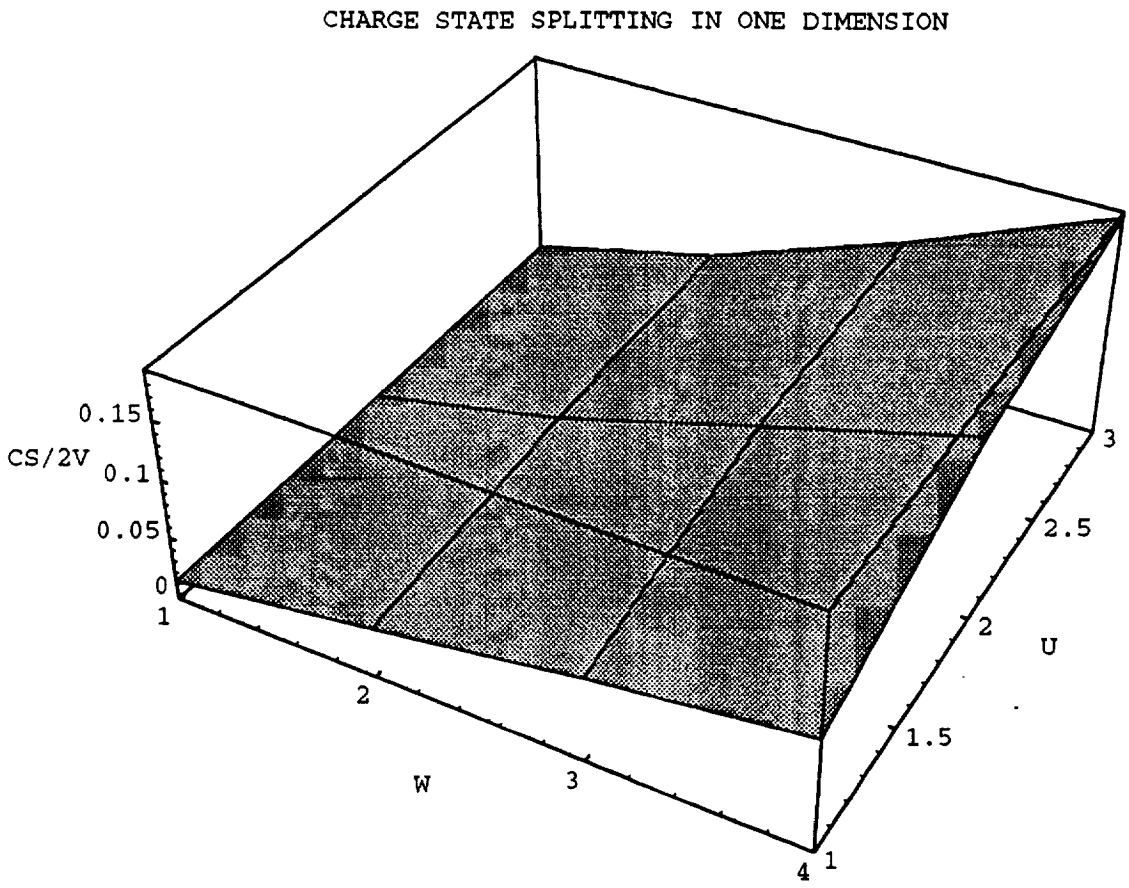


**Figure A**

**The empirical parameters chosen for this plot using the Haldane-Anderson model are $\beta$ =0.7, u=$\beta$b/(.6V), w=$\beta$a'/(.75V),V=5eV, b=4.3, and a'=11eV.**

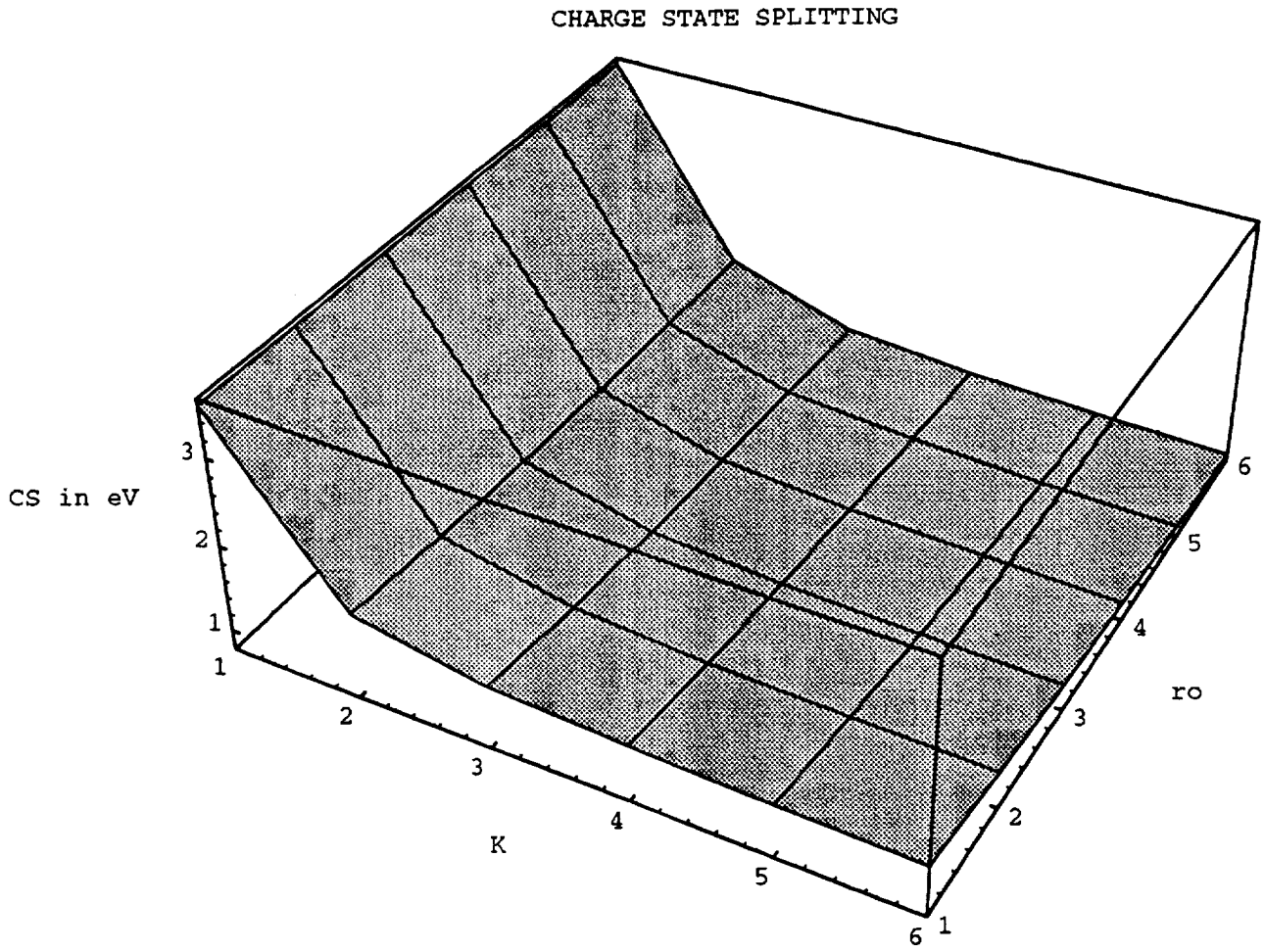


**Figure B**

**This is an atom like model with a Coulomb potenttial short range potential of range $r_o$ (which ranges from 6 to 12 Angstroms as the index goes from 1 to 6). K is the relative dielectric constant. The depth of the potential is 5 eV.**

## Deep Levels of substitutional impurities in MCT

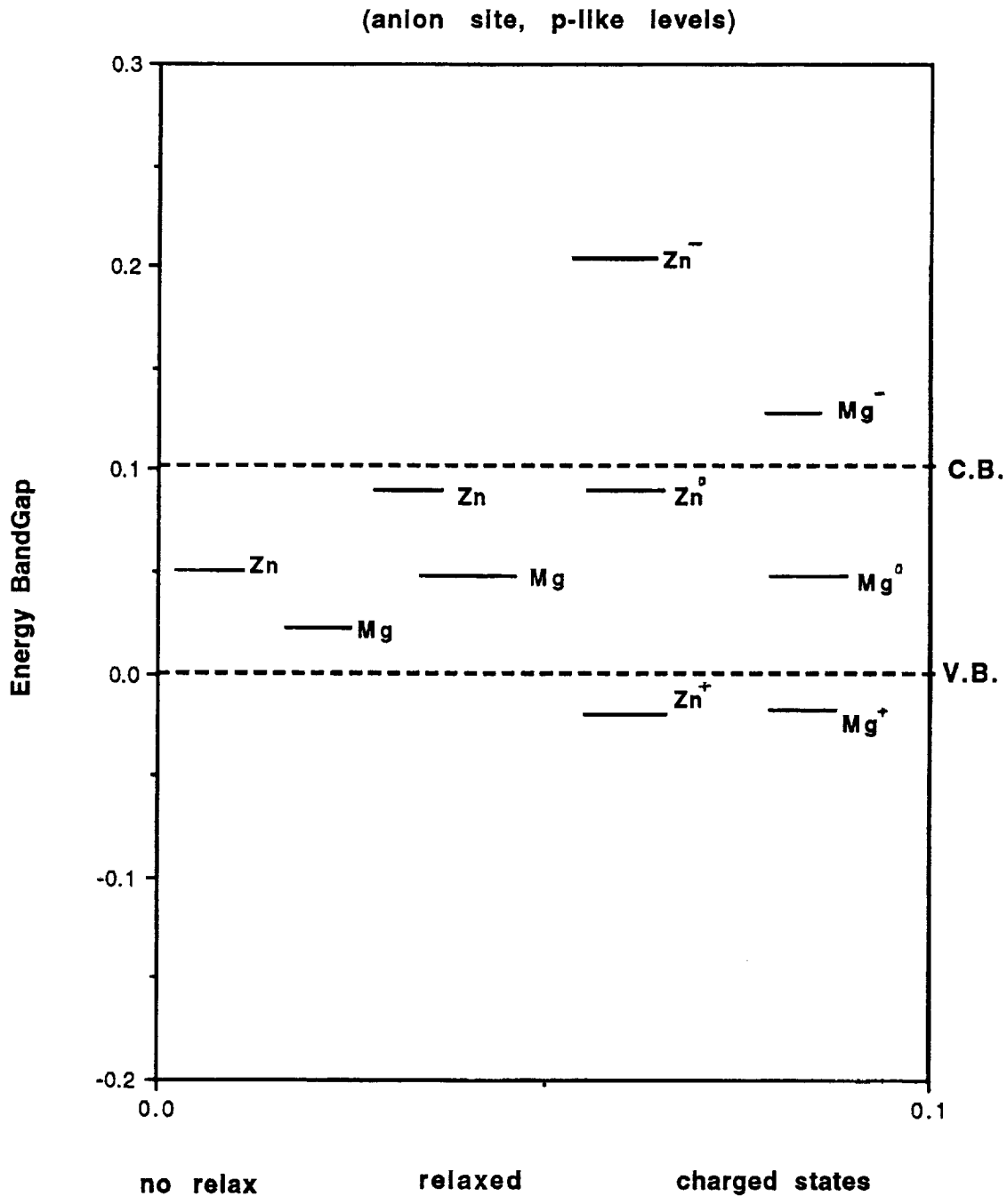


Figure 1

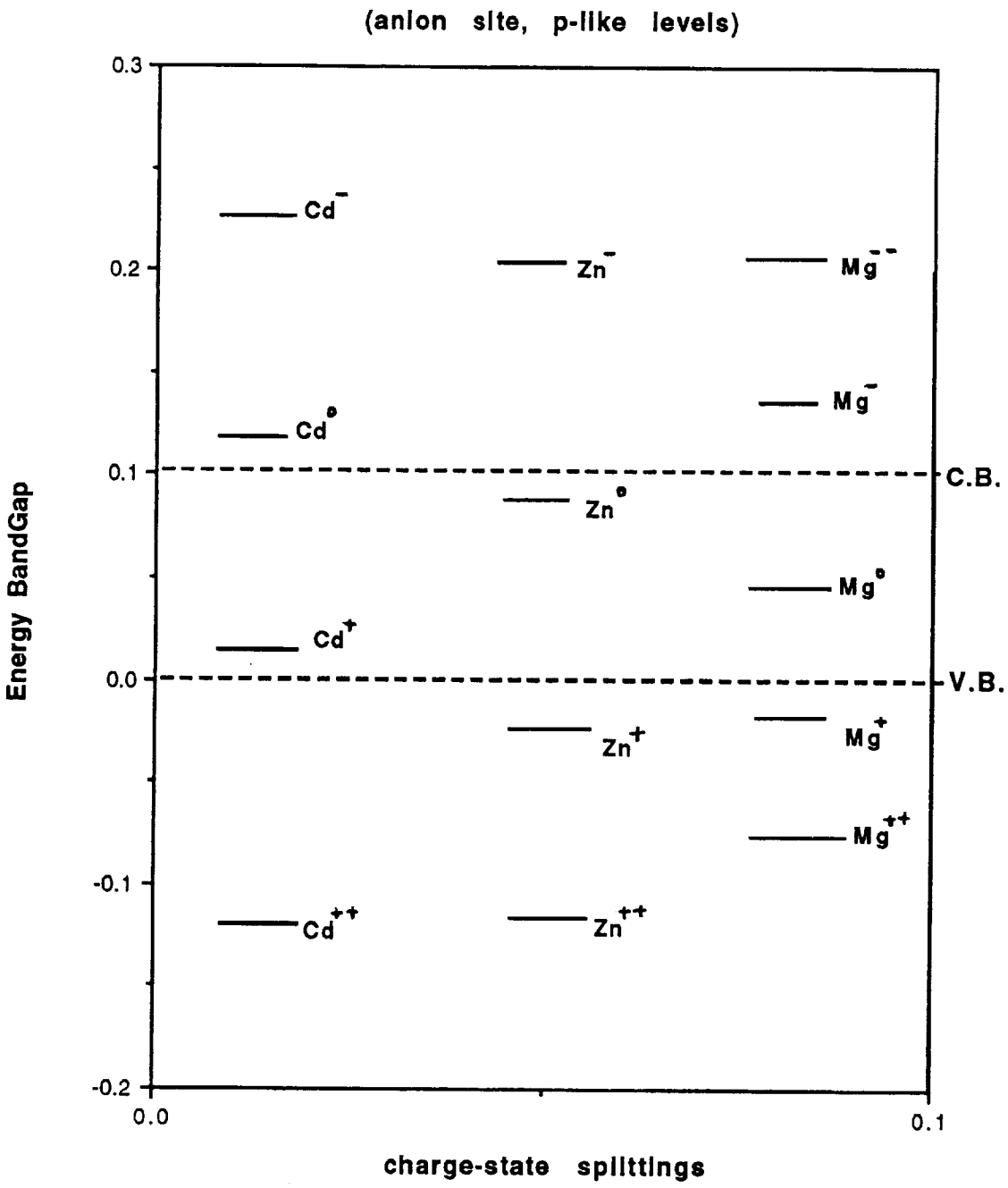
Deep Levels of substitutional impurities in MCT
(anion site, p-like levels)
Energy BandGap
charge-state splittings
0.3
0.2
0.1
0.0
-0.1
-0.2
0.0
0.1
C.B.
V.B.
Cd⁻
Zn⁻
Mg⁻⁻
Mg⁻
Cd⁰
Zn⁰
Mg⁰
Cd⁺
Zn⁺
Mg⁺
Mg⁺⁺
Cd⁺⁺
Zn⁺⁺

Figure 2

## Deep Levels of substitutional impurities in MCT

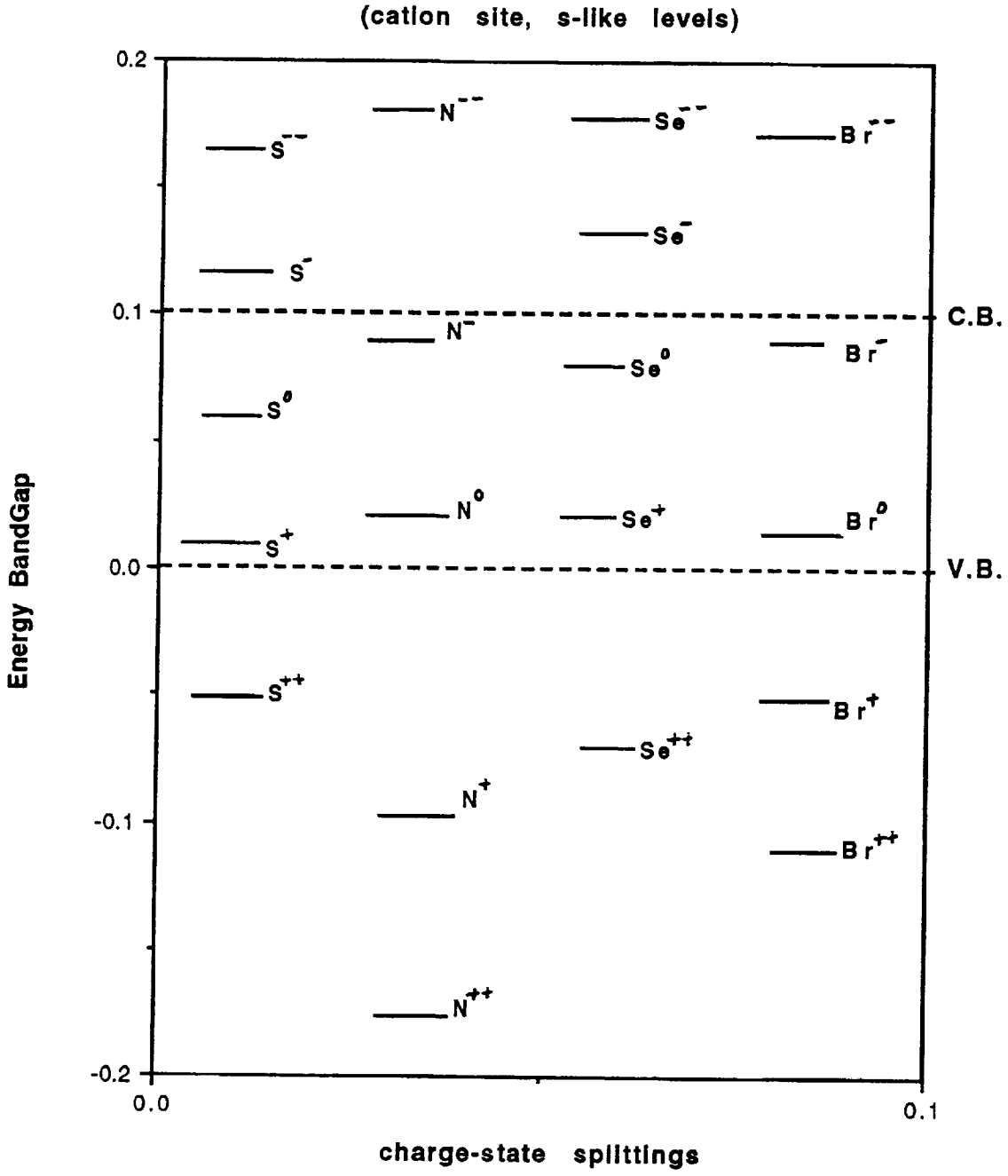


Figure 3

## Deep Levels of substitutional impurities in MZT

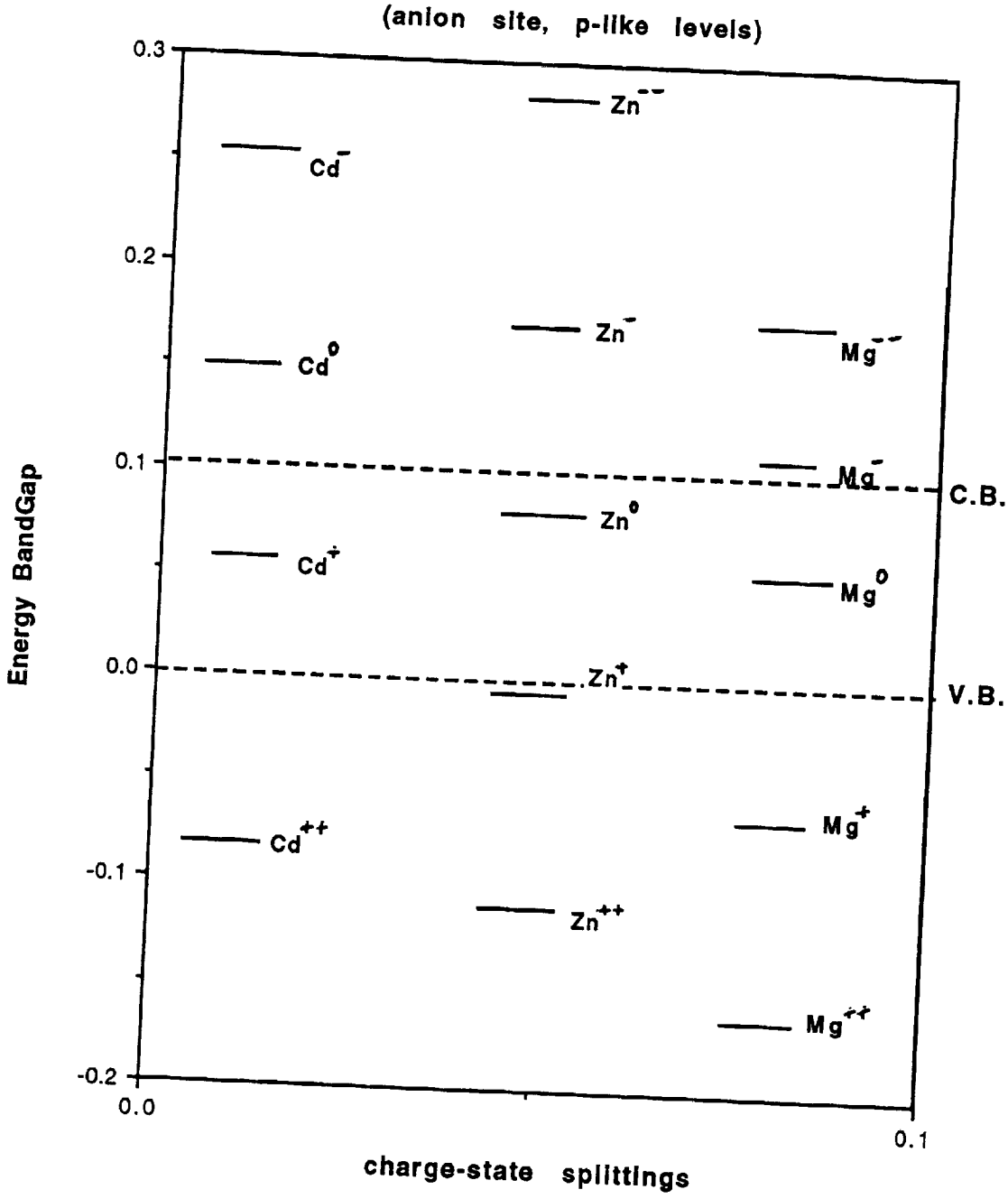


**Figure 4**

## Deep Levels of substitutional impurities in MZS

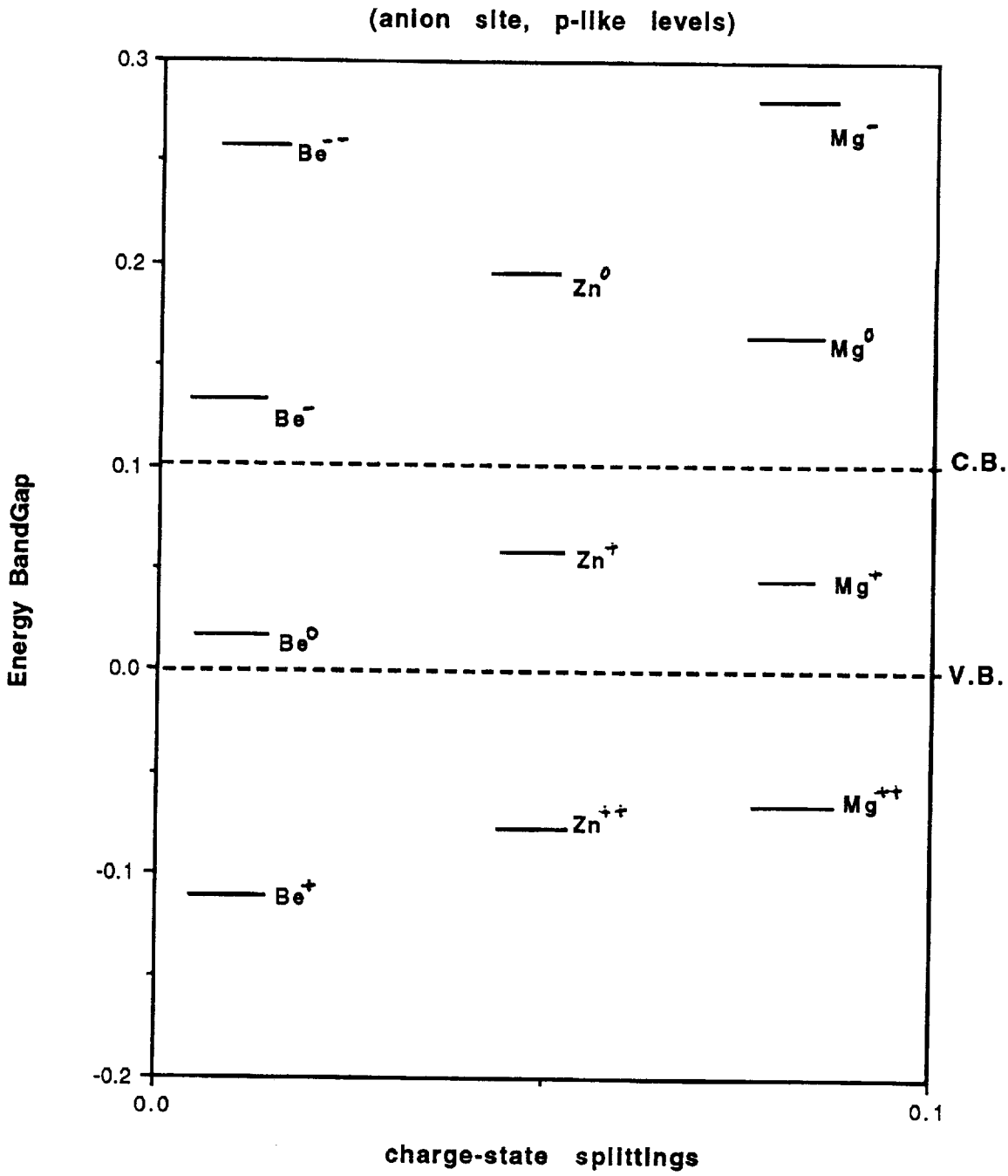


Figure 5

## Deep Levels of Interstitial Impurities in MCT

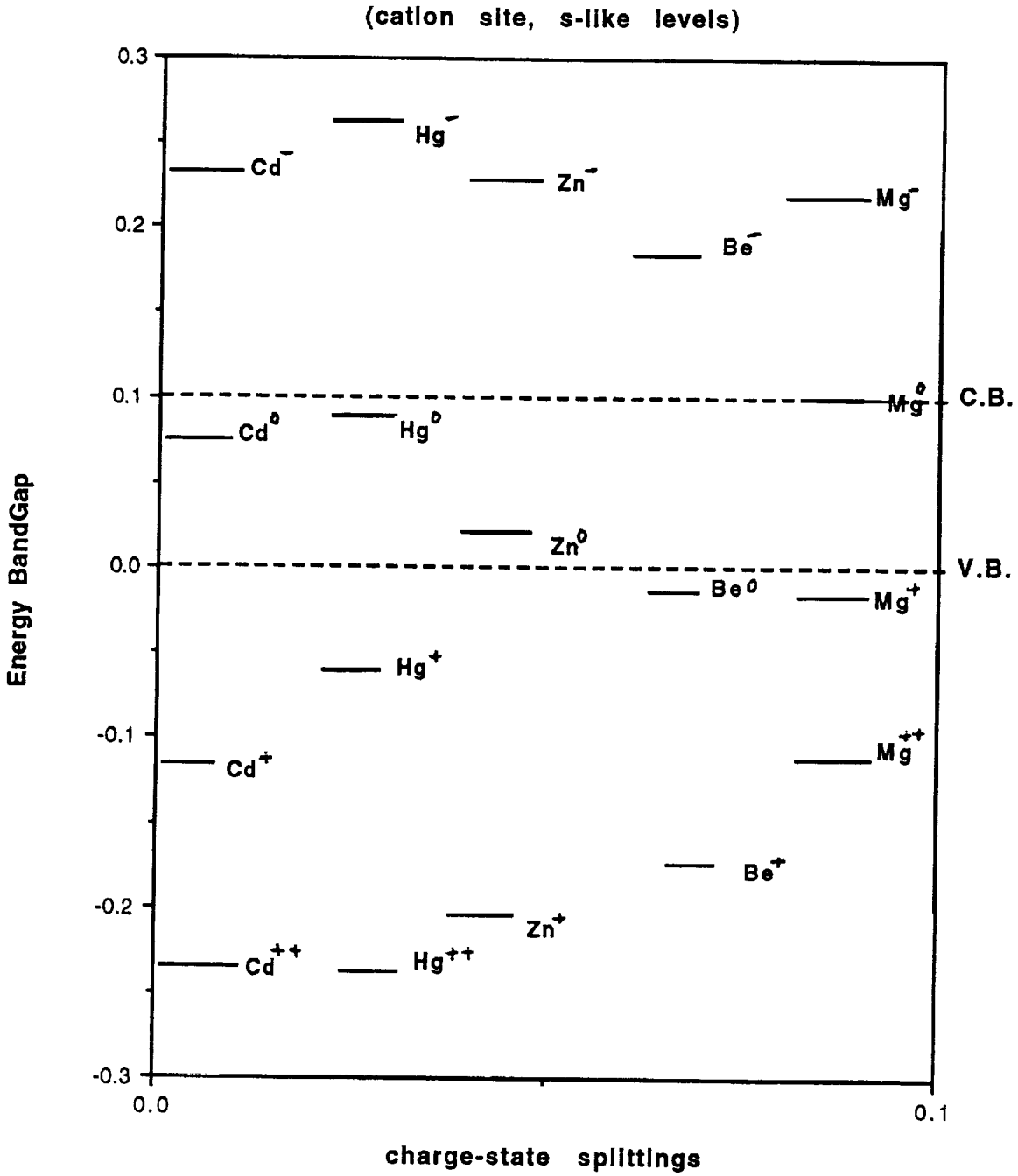


Figure 6

## Deep Levels of Interstitial Impurities in MZT

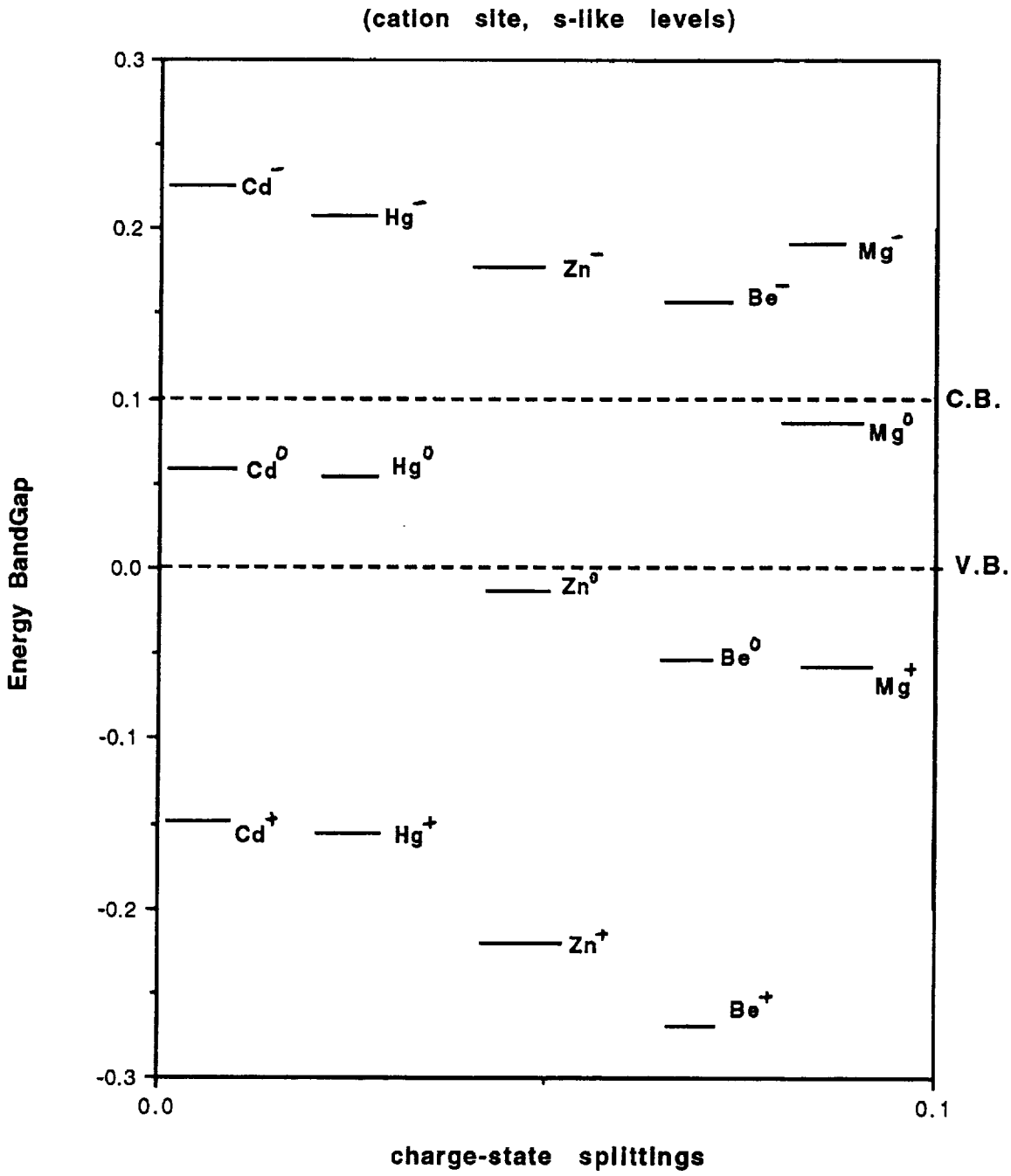


Figure 7

## Deep Levels of Interstitial Impurities in MZS

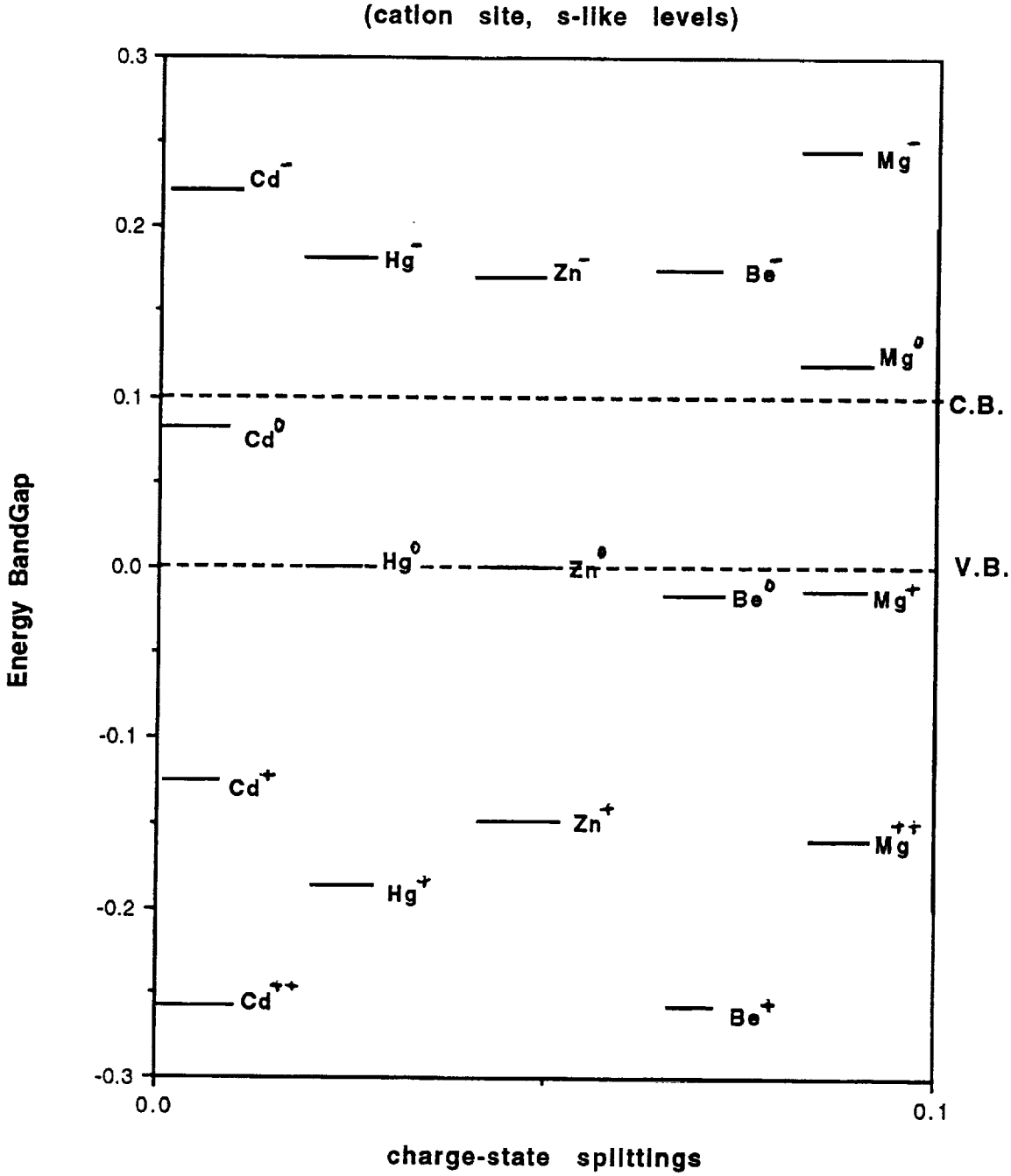


Figure 8